

A NEW CLASS OF SEMI-IMPLICIT METHODS WITH LINEAR COMPLEXITY FOR NONLINEAR FRACTIONAL DIFFERENTIAL EQUATIONS *

FANHAI ZENG[†], IAN TURNER^{†,‡}, KEVIN BURRAGE^{†,§}, AND GEORGE EM KARNIADAKIS[¶]

Abstract. We propose a new class of semi-implicit methods for solving nonlinear fractional differential equations and study their stability. Several versions of our new schemes are proved to be unconditionally stable by choosing suitable parameters. Subsequently, we develop an efficient strategy to calculate the discrete convolution for the approximation of the fractional operator in the semi-implicit method and we derive an error bound of the fast convolution. The memory requirement and computational cost of the present semi-implicit methods with a fast convolution are about $O(N \log n_T)$ and $O(Nn_T \log n_T)$, respectively, where N is a suitable positive integer and n_T is the final number of time steps. Numerical simulations, including the solution of a system of two nonlinear fractional diffusion equations with different fractional orders in two-dimensions, are presented to verify the effectiveness of the semi-implicit methods.

Key words. Fast convolution, semi-implicit methods, fractional linear multi-step methods, nonlinear fractional differential equations, complex domain integration.

AMS subject classifications. 26A33, 65M06, 65M12, 65M15, 35R11

1. Introduction. Anomalous diffusion equations have attracted considerable interest over the last decade because of their ability to model transport dynamics in complex systems [26, 28]. In these models, the underlying fractional differential equations (FDEs) are *nonlocal* and time-dependent, which may cause computational difficulties due to the nonlocality and singularity of the fractional operator [6, 2, 30, 35].

The aim of this paper is to develop a class of semi-implicit and fast time-stepping methods to efficiently solve nonlinear time-fractional FDEs. We also focus on how to reduce the memory requirement and the computational cost of the numerical methods resulting from the *nonlinearity* and *nonlocality* of nonlinear time-dependent FDEs. The *singularity* of the solution of the FDE is dealt with through the use of correction terms, a topic that is not investigated in detail in this work. The interested reader is referred to [7, 21, 39] for further details.

Semi-implicit methods have been widely applied to solve nonlinear integer-order differential equations [1, 27, 16], as these methods are efficient and have larger stability regions than explicit methods, giving rise to a linear system of equations to obtain the numerical solutions. However, semi-implicit methods for nonlinear time-fractional FDEs have not been fully addressed in the literature.

There have been some explicit and semi-implicit methods for solving fractional

*This work was supported by ARC Discovery Project DP150103675 and the MURI/ARO on “Fractional PDEs for Conservation Laws and Beyond: Theory, Numerics and Applications (W911NF-15-1-0562)”.

[†]School of Mathematical Sciences, Queensland University of Technology, Brisbane, QLD 4001, Australia (f2.zeng@qut.edu.au).

[‡]Australian Research Council Centre of Excellence for Mathematical and Statistical Frontiers, Queensland University of Technology, Brisbane, QLD 4001, Australia (i.turner@qut.edu.au).

[§]Visiting Professor, Department of Computer Science, University of Oxford, OXI 3QD, UK (kevin.burridge@qut.edu.au).

[¶]Division of Applied Mathematics, Brown University, Providence RI, 02912 (george_karniadakis@brown.edu).

differential equations proposed recently. Garrappa and his collaborator have studied explicit/semi-implicit methods for fractional ordinary differential equations (FODEs), and also investigated the stability region of these methods, see e.g. [10, 11, 12, 13, 14]. Yuste and Acedo [37] proposed an explicit difference method for linear fractional diffusion equations and a weighted average version of [37] was proposed in [36]. In 2015, Cao et al. [4] proposed a time-splitting method for nonlinear FODEs based on linear interpolation, and the stability of the method was studied numerically. Two implicit-explicit time-stepping methods, one conditionally stable and the other unconditionally stable, were proposed in [5], and stability analysis was given by following the idea in [22]. The stability region of a predictor-corrector method [8] was investigated in [13]. The objective of this work is to present a new class of semi-implicit methods for nonlinear FODEs and apply them to solve nonlinear time-fractional FPDEs. The new semi-implicit method yields a linear system with a constant coefficient matrix when it is applied to nonlinear time-fractional differential equations.

A computational difficulty of numerical methods for time-dependent FDEs is caused by the *nonlocality* of the fractional operator [2, 32]. The direct time-stepping method for the time-fractional operator $k_{-\alpha} * u(t) = \int_0^t k_{-\alpha}(t-s)u(s)ds$ yields the discrete convolution as

$$(1.1) \quad \sum_{k=0}^n \omega_{n-k} u_k, \quad 0 \leq n \leq n_T,$$

which requires $O(n_T)$ active memory and $O(n_T^2)$ operations. For the case $k_{\alpha}(t) = t^{\alpha}/\Gamma(\alpha)$, the convolution $k_{\alpha} * u(t)$ defines the fractional integral of order α for $\alpha > 0$ (or Riemann–Liouville fractional derivative of order $-\alpha$ for $\alpha < 0$), see [29, 38]. The direct calculation of (1.1) becomes computationally expensive when it is applied to discretize the time variable of high-dimensional time-fractional PDEs; see [35]. Some progress on reducing the memory requirement and computational cost for calculating (1.1) has been made, and we refer the reader to [23, 19, 17, 15, 25, 2, 35, 38], where the coefficients ω_n are obtained from interpolations and the kernel function $t^{\alpha-1}/\Gamma(\alpha)$ in the fractional operator is approximated by a sum-of-exponentials. In the semi-implicit methods analyzed in this paper, the coefficients ω_n used in (1.1) are obtained from the generating functions (see (2.5) and (2.6); and more generating functions can be found in [21]). Therefore, the fast methods in [23, 19, 17, 15, 25, 2, 35, 38] are difficult to be applied here. In [30], a fast calculation of (1.1) was developed, where ω_n is computed from generating functions that correspond to the fractional backward difference formula (see (2.5)) or implicit Runge–Kutta methods. A key idea is to re-express the weight ω_n in (1.1) as a contour integral of the form

$$(1.2) \quad \omega_n = \frac{\tau}{2\pi i} \int_C e_n(\lambda\tau) F_{\omega}(\lambda) d\lambda,$$

where τ is a time step size, and e_n and F_{ω} depend on the specific discrete convolution for the approximation of the corresponding integral operator, see Section 3 for more details. In [30], the trapezoidal rules based on the Talbot contour and the hyperbolic contour were proposed to approximate (1.2). Recently, Banjai et al. [3] have carefully analysed the Runge–Kutta-based quadrature method and extended the fast method proposed in [30] to solve linear hyperbolic problems. An equally important goal of this paper is to develop a fast algorithm to calculate the discrete convolution (1.1) appearing in the proposed semi-implicit methods.

The main contributions of this work are briefly summarised below.

- i) A new class of semi-implicit methods for nonlinear FODEs is developed. The stability of the present semi-implicit methods is investigated, and the stability criteria are given and numerically verified. Several cases of the presented semi-implicit methods are proved to be unconditionally stable and are verified by numerical simulations; see Theorems 2.1–2.3, Table 2.1, and Figure 4.1.
- ii) We reformulate the fast convolution in [30] to calculate the discrete convolutions to approximate the fractional operator. This modification makes the present fast method much easier to calculate for a wider class of discrete convolutions given by (1.1) with the coefficients ω_n defined by (2.5) or (2.6); see [21] for other choices of ω_n . An error bound of the fast convolution is obtained, depending only on the discretization error of the contour integral, see (3.20), Table 4.6, and Figure 3.1. The most important difference between our fast convolution approach and [30] is that a series of auxiliary ODEs are solved by using the *backward Euler* method, while the ODEs in [30] were solved by a multi-step method or an implicit Runge–Kutta method according to the specific discrete convolutions to approximate the fractional operator; see also [3].

We note that the use of the *backward Euler* method to solve the auxiliary ODEs attributes no additional errors to the whole truncation error of our fast method as was shown in [3, 30], which is verified by numerical simulations; see (3.20), Figure 3.1, and Table 4.6. For the fast method based on interpolation given in [23, 19, 17, 15, 25, 2, 35, 38], the auxiliary ODEs can be solved exactly, see the detailed implementation in [38].

We present several numerical simulations to verify the accuracy and efficiency of the fast method, demonstrating significant savings in memory and cost, especially when it is applied to solve high-dimensional time-fractional PDEs, see Example 4.2.

This paper is organized as follows. A new class of semi-implicit methods for nonlinear FODEs is proposed in Section 2, and the linear stability of these methods is also analyzed. A new fast implementation of the semi-implicit methods is presented in Section 3. Numerical simulations are given to verify the effectiveness of the semi-implicit and fast methods in Section 4 before the conclusion is given in the last section.

2. Semi-implicit time-stepping methods. Consider the following nonlinear FODE

$$(2.1) \quad {}_CD_{0,t}^\alpha u(t) = \lambda u(t) + f(u(t), t), \quad u(0) = u_0, \quad t \in (0, T],$$

where $0 < \alpha \leq 1$, $\lambda \in \mathbb{C}$, $Re(\lambda) < 0$, and $f(u, t)$ is a nonlinear function with respect to u , and ${}_CD_{0,t}^\alpha$ is the Caputo fractional derivative operator defined by

$$(2.2) \quad {}_CD_{0,t}^\alpha u(t) = \frac{1}{\Gamma(1-\alpha)} \int_0^t (t-s)^{-\alpha} u'(s) ds.$$

We also assume that the solution $u(t)$ to (2.1) satisfies

$$(2.3) \quad u(t) - u(0) = \sum_{n=1}^m c_n t^{\sigma_n} + t^{\sigma_{m+1}} \tilde{u}(t), \quad 0 < \sigma_n < \sigma_{n+1},$$

where $\tilde{u}(t)$ is uniformly bounded for $t \in [0, T]$. The above assumption holds in real applications, see, for example, [6, 9, 24, 20, 28], in which $\sigma_n \in \{i + j\alpha, i, j \in \mathbb{Z}^+\}$ if $f(u(t), t)$ is sufficiently smooth for $t \in [0, T]$.

2.1. Derivation of the semi-implicit methods. Denote by $t_j = j\tau$ ($j \geq 0$) the grid points, where $\tau = T/n_T$ is the stepsize, and n_T is a positive integer. Let $u_n = u(t_n)$ and denote

$$(2.4) \quad D_\tau^{(\alpha, n, m, \sigma)} u = \frac{1}{\tau^\alpha} \sum_{j=0}^n \omega_{n-j}^{(\alpha)} (u_j - u_0) + \frac{1}{\tau^\alpha} \sum_{j=1}^m w_{n,j}^{(\alpha)} (u_j - u_0),$$

where the quadrature weights $\omega_j^{(\alpha)}$ satisfy the following generating functions [21]

$$(2.5) \quad \omega(p, \alpha, \tau, z) = \left(\frac{1}{\tau} \sum_{k=1}^p \frac{1}{k} (1-z)^k \right)^\alpha = \sum_{n=0}^{\infty} \omega_n z^n = \frac{1}{\tau^\alpha} \sum_{n=0}^{\infty} \omega_n^{(\alpha)} z^n,$$

or

$$(2.6) \quad \omega(p, \alpha, \tau, z) = \left(\frac{1-z}{\tau} \right)^\alpha \sum_{k=1}^p g_{k-1}^{(\alpha)} (1-z)^{k-1} = \sum_{n=0}^{\infty} \omega_n z^n = \frac{1}{\tau^\alpha} \sum_{n=0}^{\infty} \omega_n^{(\alpha)} z^n,$$

in which $g_{p-1}^{(\alpha)}$ ($1 \leq p \leq 6$) are given by (see [10])

$$(2.7) \quad \begin{aligned} g_0^{(\alpha)} &= 1, & g_1^{(\alpha)} &= \frac{\alpha}{2}, & g_2^{(\alpha)} &= \frac{\alpha^2}{8} + \frac{5\alpha}{24}, \\ g_3^{(\alpha)} &= \frac{\alpha^3}{48} + \frac{5\alpha^2}{48} + \frac{\alpha}{8}, & g_4^{(\alpha)} &= \frac{\alpha^4}{384} + \frac{5\alpha^3}{192} + \frac{97\alpha^2}{1152} + \frac{251\alpha}{2880}, \\ g_5^{(\alpha)} &= \frac{\alpha^5}{3840} + \frac{5\alpha^4}{1152} + \frac{61\alpha^3}{2304} + \frac{401\alpha^2}{5760} + \frac{19\alpha}{288}. \end{aligned}$$

We refer readers to [21] for other choices of generating functions.

Once the quadrature weights $\omega_j^{(\alpha)}$ are given, the starting weights $w_{n,j}^{(\alpha)}$ in (2.4) are chosen such that

$$\sum_{j=0}^n \omega_{n-j}^{(\alpha)} u_j + \sum_{j=1}^m w_{n,j}^{(\alpha)} u_j = \frac{\Gamma(\sigma_r + 1)}{\Gamma(\sigma_r + 1 - \alpha)} n^{\sigma_r - \alpha}$$

for some $u(t) = t^{\sigma_r}$, $r = 1, 2, \dots, m$. We refer readers to [7, 21, 39] for more information on how to determine the starting weights and their properties.

Using the relationship ${}_C D_{0,t}^\alpha u(t) = k_{-\alpha} * (u - u(0))(t)$ and (2.3), we can apply the fractional linear multi-step method (FLMM) (2.4) to discretize the Caputo fractional derivative operator in (2.1), which yields

$$(2.8) \quad D_\tau^{(\alpha, n, m, \sigma)} u = \lambda u_n + f_n + O(\tau^p t_n^{\sigma_{m+1} - p - \alpha}) + O(\tau^{\sigma_{m+1} + 1} t_n^{-\alpha - 1}),$$

where $f_n = f(u_n, t_n)$ and $D_\tau^{(\alpha, n, m, \sigma)}$ is defined by (2.4).

Let U_n be the approximate solution of $u(t_n)$. From (2.8), we derive the following fully implicit method

$$(2.9) \quad D_\tau^{(\alpha, n, m, \sigma)} U = \lambda U_n + f(U_n, t_n),$$

where $D_\tau^{(\alpha, n, m, \sigma)}$ is defined by (2.4). We present (2.9) in order that we can compare it with the semi-implicit method developed in the following section.

Cao et al. [4] proposed two methods to linearize the nonlinear term $f(u_n, t_n)$ in (2.8) (see Eq. (2.31) in [4]). We list the two linearization approaches below:

- Extrapolation with correction terms

$$(2.10) \quad f_n = 2f_{n-1} - f_{n-2} + \sum_{j=1}^{m_f} w_{n,j}^{(f)}(f_j - f_0) + O(\tau^2 t_n^{\delta_{m_f+1}-2}),$$

where $0 < \delta_r < \delta_{r+1}$, $\delta_r \in \{\sigma_k\} \cup \{\sigma_k - \alpha\}$, and $w_{n,j}^{(f)}$ are chosen such that $f_n = 2f_{n-1} - f_{n-2} + \sum_{j=1}^{m_f} w_{n,j}^{(f)} f_j$ for $f = t^{\delta_k}$, $1 \leq k \leq m_f$.

- Taylor expansion with corrections

$$(2.11) \quad \begin{aligned} f_n \approx & f_{n-1} + \tau \partial_t f(u_{n-1}, t_{n-1}) + \sum_{j=1}^{m_1} W_{n,j}^{(1)}(f_j - f_0) \\ & + \partial_u f(u_{n-1}, t_{n-1}) \left(u_n - u_{n-1} + \sum_{j=1}^{m_2} W_{n,j}^{(2)}(u_j - u_0) \right), \end{aligned}$$

where the starting weights $W_{n,j}^{(1)}$ and $W_{n,j}^{(2)}$ are not used in this paper and the interested readers can refer to [4].

Compared with (2.11), the first approach (2.10) is much simpler. We will make a modification of (2.10) and (2.11) to derive the new semi-implicit methods. Here, we mainly focus on a modification of (2.10), which is presented below

$$(2.12) \quad f_n = f_n - E_q^{n,m_f,\delta}(f) - \kappa E_q^{n,m_u,\sigma}(u) + O(\tau^q t_n^{\delta_{m_f+1}-q}) + O(\tau^q t_n^{\sigma_{m_u}+1-q}),$$

where κ is a constant that may depend on $\partial_u f(u, t)$, and $E_q^{n,m,\sigma}(u)$ is given by

$$(2.13) \quad E_q^{n,m,\sigma}(u) = E_q^n(u) - \sum_{j=1}^m w_{n,j}^{(u)}(u_j - u_0),$$

where $\{w_{n,j}^{(u)}\}$ are chosen such that $E_q^{n,m,\sigma}(u) = 0$ for $u = t^{\sigma_r}$, $r = 1, 2, \dots, m$. Here $E_q^n(u)$ is a q th-order perturbation that is defined by

$$(2.14) \quad E_q^n(u) = \begin{cases} u_n - u_{n-1}, & q = 1, \\ u_n - 2u_{n-1} + u_{n-2}, & q = 2. \end{cases}$$

We can interpret $E_q^n(u)$ as a penalty term that balances the stability and accuracy of the proposed method. Note that $E_q^n(u) = O(\tau^q)$ if $u(t)$ is a smooth function for $t \in [0, T]$. Higher-order perturbations $E_q^n(u) = O(\tau^q)$ of order $q \geq 3$ can be constructed, which are not investigated here. In real applications, the solution to the considered FDE is often non-smooth, and therefore correction terms $\sum_{j=1}^{m_u} w_{n,j}^{(u)}(u_j - u_0)$ are added in (2.13), such that $E_q^{n,m,\sigma}(u)$ has smaller magnitude than $E_q^n(u)$.

Combining (2.8) and (2.12), we have

$$(2.15) \quad D_\tau^{(\alpha,n,m,\sigma)} u = \lambda u_n + f_n - E_q^{n,m_f,\delta}(f) - \kappa E_q^{n,m_u,\sigma}(u) + R^n,$$

where the truncation error R^n satisfies

$$(2.16) \quad R^n = O(\tau^p t_n^{\sigma_{m+1}-p-\alpha}) + O(\tau^{\sigma_{m+1}+1} t_n^{-\alpha-1}) + O(\tau^q t_n^{\delta_{m_f+1}-q}) + O(\tau^q t_n^{\sigma_{m_u}+1-q}).$$

From (2.15), we obtain the following semi-implicit scheme

$$(2.17) \quad D_\tau^{(\alpha, n, m, \sigma)} U = \lambda U_n + F_n - E_q^{n, m_f, \delta}(F) - \kappa E_q^{n, m_u, \sigma}(U),$$

where $F_n = f(U_n, t_n)$, $E_q^{n, m, \sigma}$ is defined by (2.13), and $D_\tau^{(\alpha, n, m, \sigma)}$ is defined by (2.4).

We can also make a modification of (2.11) to derive another semi-implicit method, i.e., we just need to replace $\partial_u f(u_{n-1}, t_{n-1})u_n$ in (2.11) with

$$-\kappa u_n + (\kappa + \partial_u f(u_{n-1}, t_{n-1}))(u_n - E_q^{n, m_u, \sigma}(u)).$$

From (2.12) and the above expression, we obtain the second semi-implicit method

$$(2.18) \quad \begin{aligned} D_\tau^{(\alpha, n, m, \sigma)} U &= (\lambda - \kappa)U_n + F_{n-1} + \tau \partial_t f(U_{n-1}, t_{n-1}) + \sum_{j=1}^{m_1} W_{n,j}^{(1)}(F_j - F_0) \\ &+ \partial_u f(U_{n-1}, t_{n-1}) \left(-U_{n-1} + \sum_{j=1}^{m_2} W_{n,j}^{(2)}(U_j - U_0) \right) \\ &+ (\kappa + \partial_u f(U_{n-1}, t_{n-1}))(U_n - E_q^{n, m_u, \sigma}(U)). \end{aligned}$$

If all the correction terms in (2.17) and (2.18) are omitted, both modified methods reduce to the same method for a linear problem for $q = 2$. Compared with the first method (2.17), the second method (2.18) seems much more complicated and involves using partial derivatives of the nonlinear term $f(u, t)$. In the remaining sections of this paper, we mainly focus on the theoretical analysis of the first method (2.17) and its application to solving nonlinear FDEs.

2.2. Linear stability. We investigate the linear stability of the method (2.17) in this subsection. Let $f(u, t) = \rho u$. For simplicity, we first drop all the correction terms since they do not affect the stability of the proposed method under some suitable conditions. In such a case, (2.17) becomes

$$(2.19) \quad \frac{1}{\tau^\alpha} \sum_{j=0}^n \omega_{n-j}^{(\alpha)}(U_j - U_0) = (\lambda + \rho)U_n - (\rho + \kappa)E_q^n(U),$$

where $\omega_n^{(\alpha)}$ satisfies $\omega(p, \alpha, 1, z) = \sum_{n=0}^{\infty} \omega_n^{(\alpha)} z^n$, and $\omega(p, \alpha, \tau, z)$ is defined by (2.5) or (2.6).

In the following, we analyze the stability of (2.19) for $q = 2$. Eq. (2.19) becomes

$$(2.20) \quad \frac{1}{\tau^\alpha} \sum_{j=0}^n \omega_{n-j}^{(\alpha)}(U_j - U_0) = (\lambda - \kappa)U_n + (\rho + \kappa)(2U_{n-1} - U_{n-2}).$$

For $q = 1$, we need only to replace $(\rho + \kappa)(2U_{n-1} - U_{n-2})$ in (2.20) with $(\rho + \kappa)U_{n-1}$.

Define

$$(2.21) \quad \mathbb{S} = \mathbb{C} \setminus \left\{ \xi | \xi^\alpha = \frac{\omega(p, \alpha, 1, z)}{(\lambda + \rho) - (\rho + \kappa)(1 - z)^q}, |z| \leq 1 \right\},$$

where $\omega(p, \alpha, \tau, z)$ is defined by (2.5) or (2.6).

According to [4, 22], we have the following two theorems, the proofs of which are given in Appendix A.

THEOREM 2.1. If $\tau \in \mathbb{S}$ with \mathbb{S} defined by (2.21), then method (2.19) for the model problem ${}_CD_{0,t}^\alpha u(t) = (\lambda + \rho)u(t)$ is stable.

THEOREM 2.2. If $\tau \in \mathbb{S}$ with \mathbb{S} defined by (2.21), $\sigma_m < \alpha + p$, $\sigma_{m_u}, \delta_{m_f} < q$, then method (2.17) for the model problem ${}_CD_{0,t}^\alpha u(t) = (\lambda + \rho)u(t)$ is stable.

REMARK 2.1. Let $\alpha > 0$ be a rational number, i.e., $\alpha = n/r$, r, n are positive integers and $\gcd(r, n) = 1$. Define the polynomial

$$P(\hat{z}) = \hat{z}^n \sum_{k=1}^p g_{k-1}^{(\alpha)} \hat{z}^{r(k-1)} + \tau^\alpha (\rho + \kappa) \hat{z}^{qr} - \tau^\alpha (\lambda + \rho), \quad \hat{z} = (1 - z)^{1/r}, \quad |z| \leq 1,$$

where $g_k^{(\alpha)}$ are defined by (2.7). If the generating function (2.6) is used and $P(\hat{z})$ has no root in the domain defined by $\hat{z} = (1 - z)^{1/r}$, $|z| \leq 1$, then the method (2.19) is stable.

Several special cases of (2.21) are given in the following theorem, the proof of which is provided in Appendix B.

THEOREM 2.3. Suppose that $\lambda < 0, \rho \leq 0$. For $p = 1, 2$, the method (2.19) is unconditionally stable if

$$(2.22) \quad \kappa > \begin{cases} (\lambda - \rho)/2, & q = 1, \\ (\lambda - 3\rho)/4, & q = 2. \end{cases}$$

In our numerical simulations, we will apply the second-order generalized Newton-Gregory formula to discretize the fractional derivative operators in the considered FDEs, i.e., $\omega(p, \alpha, \tau, z)$ is chosen as $\tau^\alpha \omega(p, \alpha, \tau, z) = (1 - z)^\alpha (1 + \frac{\alpha}{2} - \frac{\alpha}{2}z)$. Therefore, we first present the stability interval of the method (2.19) in Table 2.1, where we set $p = q = 2$. From Table 2.1, we have the following observations:

- For a fixed fractional order α , the stability interval increases as κ increases.
- For a small κ , the stability interval may be very small when α tends to zero; $\kappa = 0$ corresponds to the extrapolation method in [4].
- There exists a $\kappa_0 \geq 0$, such that the method (2.19) is stable for any $\tau > 0$ and $\alpha \in (0, 1]$ if $\kappa \geq \kappa_0$. For the case shown in Table 2.1, $\kappa_0 = 1.25$, which verifies (2.22).

TABLE 2.1

Stability interval of (2.20) with a second-order generating function $\omega(p, \alpha, \tau, z) = \tau^{-\alpha}(1 - z)^\alpha(1 + \frac{\alpha}{2} - \frac{\alpha}{2}z)$ for different fractional orders α and κ , $\lambda = -1, \rho = -2$.

κ	$\alpha = 0.1$	$\alpha = 0.2$	$\alpha = 0.5$	$\alpha = 0.9$
0	$(0, 5.31 \times 10^{-7})$	$(0, 1.59 \times 10^{-3})$	$(0, 1.80 \times 10^{-1})$	$(0, 6.83 \times 10^{-1})$
0.2	$(0, 3.04 \times 10^{-6})$	$(0, 3.81 \times 10^{-3})$	$(0, 2.55 \times 10^{-1})$	$(0, 8.28 \times 10^{-1})$
0.4	$(0, 2.51 \times 10^{-5})$	$(0, 1.10 \times 10^{-2})$	$(0, 3.89 \times 10^{-1})$	$(0, 1.05 \times 10^0)$
0.6	$(0, 3.67 \times 10^{-4})$	$(0, 4.19 \times 10^{-2})$	$(0, 6.66 \times 10^{-1})$	$(0, 1.41 \times 10^0)$
0.8	$(0, 1.45 \times 10^{-2})$	$(0, 2.63 \times 10^{-1})$	$(0, 1.39 \times 10^0)$	$(0, 2.12 \times 10^0)$
1.0	$(0, 5.19 \times 10^0)$	$(0, 4.98 \times 10^0)$	$(0, 4.50 \times 10^0)$	$(0, 4.08 \times 10^0)$
1.2	$(0, 5.07 \times 10^7)$	$(0, 1.56 \times 10^4)$	$(0, 1.13 \times 10^2)$	$(0, 2.44 \times 10^1)$
1.24	$(0, 4.95 \times 10^{14})$	$(0, 4.86 \times 10^7)$	$(0, 2.81 \times 10^3)$	$(0, 1.46 \times 10^2)$
1.25	$(0, \infty)$	$(0, \infty)$	$(0, \infty)$	$(0, \infty)$
1.26	$(0, \infty)$	$(0, \infty)$	$(0, \infty)$	$(0, \infty)$
1.40	$(0, \infty)$	$(0, \infty)$	$(0, \infty)$	$(0, \infty)$

Next, we plot the stability region of the method (2.20) under some restrictions. Let $\rho = \gamma\lambda, \kappa = -\theta\rho = -\theta\gamma\lambda$, and $\xi = \tau^\alpha\lambda$. Then, the stability domain of the method

(2.19) can be expressed by

$$(2.23) \quad \mathbb{D} = \mathbb{C} \setminus \left\{ \xi \mid \xi = \frac{\omega(p, \alpha, 1, z)}{(1 + \gamma) - \gamma(1 - \theta)(1 - z)^q}, |z| \leq 1 \right\}.$$

Figure 2.1 displays the stability region defined by (2.23) when $Re(\kappa) < Re(\lambda - 3\rho)/4$ and $\omega(2, \alpha, 1, z) = (1 - z)^\alpha(1 + \frac{\alpha}{2} - \frac{\alpha}{2}z)$. We see that as θ (or $Re(\kappa)$) increases, the stability region (the shaded area) becomes larger for a fixed α .

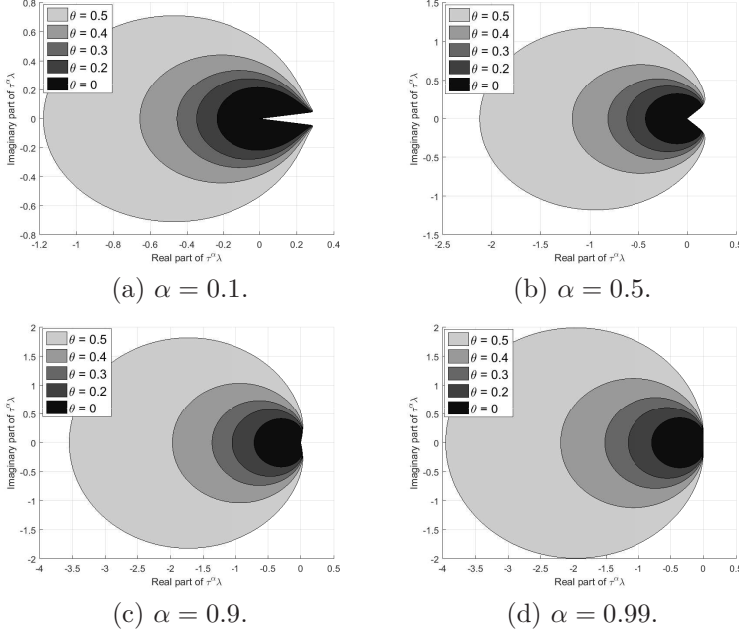


FIG. 2.1. Stability region (the shaded area) of the method (2.19), $q = 2$, $\rho = 2\lambda$, $\kappa = -\theta\rho$.

Figure 2.2 displays the stability region when $Re(\kappa) > Re(\lambda - 3\rho)/4$. We again observe that the stability region becomes large as θ (or $Re(\kappa)$) increases and the stability region contains the whole negative axis, which verifies Theorem 2.3.

Figure 2.3 shows the stability region of the method (2.19) when the generalized Newton–Gregory formula of order p is applied, see (2.6). For $\theta = 0.5$, we have $Re(\kappa) < Re(\lambda - 3\rho)/4$; the method is conditionally stable and the stability region becomes large as p increases. For $Re(\kappa) > Re(\lambda - 3\rho)/4$, i.e., $\theta = 0.63$, the stability region contains the negative axis, see Figure 2.4. For other fractional orders $\alpha \in (0, 1]$, we have similar results. If the fractional backward difference formula (FBDF) of order p is applied, the stability of the method (2.19) shows similar behavior as shown in Figures 2.2–2.4, hence these results are not shown here.

2.3. System of equations. In this subsection, we extend the semi-implicit method (2.17) to the following system of equations

$$(2.24) \quad {}_CD_{0,t}^{\vec{\alpha}} \vec{u}(t) = \mathbf{A} \vec{u}(t) + \vec{f}(\vec{u}(t), t), \quad \vec{u}(0) = \vec{u}_0, \quad t \in (0, T],$$

where $\vec{u}(t) = (u^{(1)}(t), \dots, u^{(d)}(t))^T$, $\vec{\alpha} = (\alpha^{(1)}, \dots, \alpha^{(d)})^T$, $\alpha^{(j)} \in (0, 1]$, $\mathbf{A} \in \mathbb{C}^{d \times d}$, ${}_CD_{0,t}^{\vec{\alpha}} \vec{u}(t) = ({}_CD_{0,t}^{\alpha^{(1)}} u^{(1)}(t), \dots, {}_CD_{0,t}^{\alpha^{(d)}} u^{(d)}(t))^T$, $\vec{f}(\vec{u}, t) = (f^{(1)}(\vec{u}, t), \dots, f^{(d)}(\vec{u}, t))^T$, $f^{(j)}(\vec{u}, t) = f^{(j)}(u^{(1)}, \dots, u^{(d)}, t)^T$, and $d \in \mathbb{N}$.

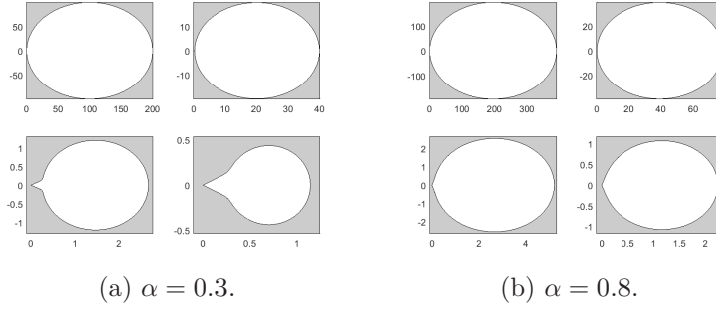


FIG. 2.2. Stability region (the shaded area) of the method (2.19), $q = 2$, $\rho = 2\lambda$, $\kappa = -\theta\rho$, $\theta = 0.626, 0.63, 0.8, 0.7$ in clockwise order starting from the upper left.

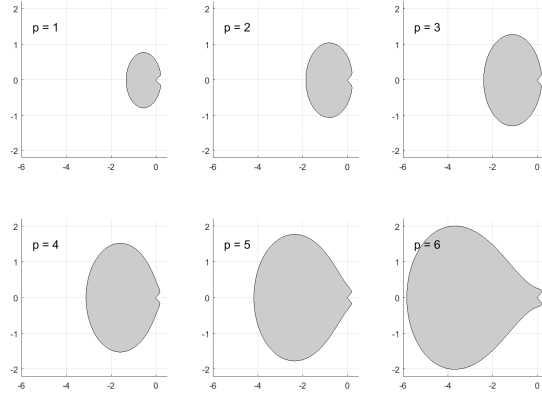


FIG. 2.3. Stability region of the method (2.19) based on generalized Newton-Gregory formula of order p , $\alpha = 0.4$, $q = 2$, $\rho = 2\lambda$, $\kappa = -0.5\rho$.

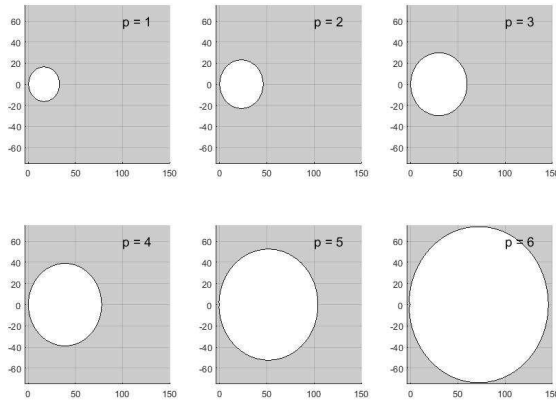


FIG. 2.4. Stability region of (2.19) based on the FBDF- p , $\alpha = 0.4$, $q = 2$, $\rho = 2\lambda$, $\kappa = -0.63\rho$.

Let $\vec{U}_n = (U_n^{(1)}, U_n^{(2)}, \dots, U_n^{(d)})^T$ be the approximate solution of $\vec{u}(t_n)$. Similar to (2.17), we directly present the semi-implicit method for (2.24) as follows:

$$(2.25) \quad D_\tau^{(\vec{\alpha}, n, \vec{m}, \vec{\sigma})} \vec{U} = \mathbf{A} \vec{U}_n + \vec{F}_n - E_q^{n, \vec{m}_f, \vec{\delta}}(\vec{F}) - \kappa E_q^{n, \vec{m}_u, \vec{\sigma}}(\vec{U}),$$

where $\vec{m} = (m^{(1)}, \dots, m^{(d)})^T$, $\vec{\sigma} = (\sigma^{(1)}, \dots, \sigma^{(d)})^T$, $F_n^{(j)} = f^{(j)}(\vec{U}_n, t_n)$, $D_\tau^{(\vec{\alpha}, n, \vec{m}, \vec{\sigma})} \vec{U} = (D_\tau^{(\alpha^{(1)}, n, m^{(1)}, \sigma^{(1)})} U^{(1)}, \dots, D_\tau^{(\alpha^{(d)}, n, m^{(d)}, \sigma^{(d)})} U^{(d)})^T$, $D_\tau^{(\alpha^{(j)}, n, m^{(j)}, \sigma^{(j)})}$ is defined by (2.4), $E_q^{n, \vec{m}, \vec{\sigma}}(\vec{U}) = (E_q^{n, m^{(1)}, \sigma^{(1)}}(U^{(1)}), \dots, E_q^{n, m^{(d)}, \sigma^{(d)}}(U^{(d)}))^T$, $E_q^{n, m, \sigma}$ is defined by (2.13), and κ is a $d \times d$ matrix.

Next, we analyse the linear stability of (2.25). Let $\vec{f} = \mathbf{B} \vec{u}$, $\mathbf{B} \in \mathbb{C}^{d \times d}$ and omit all the correction terms in (2.25). Then we obtain

$$(2.26) \quad D_\tau^{(\vec{\alpha}, n, \vec{m}, \vec{\sigma})} \vec{U} = (\mathbf{A} + \mathbf{B}) \vec{U}_n - (\kappa + \mathbf{B}) E_q^n(\vec{U}).$$

Similar to the stability analysis given in the previous subsection, we can obtain that the method (2.26) is stable if

$$(2.27) \quad \det(\text{diag}(\vec{\omega}(p, \vec{\alpha}, 1, z)) - \text{diag}(\tau^{\vec{\alpha}}) [(\mathbf{A} + \mathbf{B}) - (\mathbf{B} + \kappa)(1 - z)^q]) \neq 0, \quad |z| \leq 1,$$

where $\vec{\omega}(p, \vec{\alpha}, 1, z) = (\omega(p, \alpha^{(1)}, 1, z), \dots, \omega(p, \alpha^{(d)}, 1, z))^T$, $\tau^{\vec{\alpha}} = (\tau^{\alpha^{(1)}}, \dots, \tau^{\alpha^{(d)}})^T$, $\sigma_{m^{(i)}}^{(i)} < \alpha^{(i)} + p$, $\sigma_{m_u^{(i)}}^{(i)}, \delta_{m_f^{(i)}}^{(i)} < q$, $1 \leq i \leq d$.

The matrix κ plays an important role in the stability of the method (2.25). From (2.11), we find that κ may depend on the Jacobian of $\vec{f}(\vec{u}, t)$ with respect to \vec{u} . It is much more difficult to present an explicit criterion as shown in Theorem 2.3 for a system equations. However, we can deduce that the stability of the method (2.26) can be enhanced if κ is positive definite for $q = 1, 2$ with the generating function (2.6) for $p = 1, 2$ applied. For example, let $q = 1$, $p = 1$ or 2 , $\vec{U}_0 = \vec{0}$, and choose a matrix κ such that $\kappa + \mathbf{B}$ is symmetric and positive definite. Then

$$(2.28) \quad \begin{aligned} & \sum_{n=1}^M (\vec{U}_n)^T D_\tau^{(\vec{\alpha}, n, \vec{m}, \vec{\sigma})} \vec{U} - \sum_{n=1}^M (\vec{U}_n)^T (\mathbf{A} + \mathbf{B}) \vec{U}_n \\ &= - \sum_{n=1}^M (\vec{U}_n)^T (\kappa + \mathbf{B}) E_1^n(\vec{U}) \leq -\frac{1}{2} (\vec{U}_M)^T (\kappa + \mathbf{B}) \vec{U}_M. \end{aligned}$$

If $\mathbf{A} + \mathbf{B}$ is negative definite, then (2.28) implies

$$(2.29) \quad 2 \sum_{n=1}^M (\vec{U}_n)^T D_\tau^{(\vec{\alpha}, n, \vec{m}, \vec{\sigma})} \vec{U} - 2 \sum_{n=1}^M (\vec{U}_n)^T (\mathbf{A} + \mathbf{B}) \vec{U}_n + (\vec{U}_M)^T (\kappa + \mathbf{B}) \vec{U}_M \leq 0.$$

Using $\sum_{n=1}^M (\vec{U}_n)^T D_\tau^{(\vec{\alpha}, n, \vec{m}, \vec{\sigma})} \vec{U} \geq 0$ (see [33]) yields $\vec{U}_n = \vec{0}$.

A practical option can be $\kappa = \text{diag}(\kappa_1, \kappa_2, \dots, \kappa_d)$, $\kappa_i \geq 0$, which is used in the numerical simulations. From (2.28), we see that $\kappa = \text{diag}(\kappa_1, \kappa_2, \dots, \kappa_d)$ can significantly enhance the stability of (2.26) when $\kappa_i \geq 0$ is sufficiently large for $q = 1, 2$. Next, we focus on the other important task of developing a fast method to calculate the discrete convolutions in the semi-implicit methods.

3. Fast implementation. In this section, we generalize and extend the approach in [30] to calculate the discrete convolution (1.1) originating from the discretization of the fractional integral and derivative operators, where ω_n are the coefficients of the generating function $F_\omega(\delta(\xi)/\tau)$, i.e., $F_\omega(\delta(\xi)/\tau) = \sum_{n=0}^{\infty} \omega_n \xi^n$, which has been discussed in the previous section. In [30], $\delta(\xi)$ is related to the linear multi-step method for the first-order initial value problem. In the present fast method, we assume $\delta(\xi) = 1 - \xi$, i.e., $\delta(\xi)$ corresponds to the backward Euler method.

3.1. Review of the existing method. We first recall the fast method proposed in [30]. The key idea is to re-express the coefficient ω_n in (1.1) using the integral formula, and then approximate it using numerical quadrature.

By Cauchy's integral formula, we have

$$(3.1) \quad F_\omega(\delta(\xi)/\tau) = \sum_{n=0}^{\infty} \omega_n \xi^n = \frac{1}{2\pi i} \int_{\mathcal{C}} \left(\frac{\delta(\xi)}{\tau} - \lambda \right)^{-1} F_\omega(\lambda) d\lambda,$$

where \mathcal{C} is a suitable contour. Define $e_n(z)$ as

$$(3.2) \quad (\delta(\xi) - z)^{-1} = \sum_{n=0}^{\infty} e_n(z) \xi^n.$$

Then ω_n can be expressed by

$$(3.3) \quad \omega_n = \frac{\tau}{2\pi i} \int_{\mathcal{C}} e_n(\lambda\tau) F_\omega(\lambda) d\lambda.$$

Inserting (3.3) into (1.1) yields

$$(3.4) \quad D_\tau^{(\alpha,n)} u = \sum_{j=0}^n \omega_{n-j} u_j = \frac{\tau}{2\pi i} \sum_{j=0}^n \int_{\mathcal{C}} e_{n-j}(\lambda\tau) F_\omega(\lambda) u_j d\lambda.$$

When the integral on the right-hand-side of the above equation is approximated by a suitable quadrature method, we have the fast convolution developed in [30].

The fractional backward difference formula (FBDF) and implicit Runge-Kutta method were investigated in [30]. For the FBDF of order p (FBDF- p), one has $\delta(\xi) = \sum_{k=1}^p \frac{1}{k} (1 - \xi)^k$ and $F_\omega(\lambda) = \lambda^\alpha$, and the corresponding $e_n(z)$ in (3.2) for $p = 1, 2$ is given by

$$(3.5) \quad e_n(z) = \begin{cases} (1 - z)^{-1-n}, & \text{FBDF-1,} \\ \frac{1}{1+2z} ((2 - \sqrt{1+2z})^{-1-n} - (2 + \sqrt{1+2z})^{-1-n}), & \text{FBDF-2.} \end{cases}$$

It seems much more complicated to obtain $e_n(z)$ for FBDF- p with $p \geq 3$.

Next, we simplify the method in [30], that is, we will always have $e_n(z) = (1 - z)^{-1-n}$ used in (3.2), and $F_\omega(\lambda)$ in (3.3) is related to a fractional linear multi-step method (FLMM) that discretizes the fractional integral or Riemann-Liouville (RL) fractional derivative operator, which will be given later.

3.2. A new fast convolution. We consider (1.1) with the coefficients ω_n derived from the FBDF- p ($1 \leq p \leq 6$) for the fractional integral and RL derivative operators, i.e., the coefficients ω_n satisfy (2.5).

Let $\delta(\xi) = 1 - \xi$ and repeat the procedures (3.1)–(3.3). Then the coefficient ω_n in (2.5) can also be expressed by

$$(3.6) \quad \omega_n = \frac{\tau}{2\pi i} \int_{\mathcal{C}} e_n(\lambda\tau) F_\omega(\lambda) d\lambda = \frac{\tau}{2\pi i} \int_{\mathcal{C}} (1 - \lambda\tau)^{-1-n} F_\omega(\lambda) d\lambda,$$

where \mathcal{C} is a contour that surrounds the pole $\lambda = \frac{1}{\tau}$ of $e_n(\lambda\tau)$ and $F_\omega(\lambda)$ is given by

$$(3.7) \quad F_\omega(\lambda) = \omega(p, \alpha, \tau, 1 - \tau\lambda) = \lambda^\alpha \left(\sum_{k=1}^p \frac{1}{k} (\tau\lambda)^{k-1} \right)^\alpha.$$

By choosing a suitable contour, (3.6) can be approximated with high accuracy. As was done in [30], we can apply the trapezoidal rule based on either a hyperbolic contour or a Talbot contour to approximate (3.6), which is given by

$$(3.8) \quad \omega_n \approx \hat{\omega}_n = \text{Im} \left(\tau \sum_{k=-N}^{N-1} w_k^{(\ell)} (1 - \lambda_k^{(\ell)} \tau)^{-1-n} F_\omega(\lambda_k^{(\ell)}) \right),$$

where the quadrature points $\lambda_k^{(\ell)}$ and weights $w_k^{(\ell)}$ are defined later in this section, see (3.14) or (3.15). If ω_n in (1.1) is defined by (2.6), then $F_\omega(\lambda)$ in (3.6) is given by

$$(3.9) \quad F_\omega(\lambda) = \omega(p, \alpha, \tau, 1 - \tau\lambda) = \lambda^\alpha \sum_{k=0}^{p-1} g_k^{(\alpha)} (\tau\lambda)^k.$$

We now present our fast method for calculating (1.1) in Algorithm 1.

Our goal below is to determine the quadrature points $\lambda_k^{(\ell)}$ and weights $w_k^{(\ell)}$ in (3.11), such that $\hat{u}_n^{(\ell)}$ is a good approximation of $u_n^{(\ell)}$ for any $n \geq n_0$. The trapezoidal rule based on the Talbot contour [30, 34] or hyperbolic contour [18, 30] has been applied to approximate $\frac{1}{2\pi i} \int_{\Gamma_\ell} e_{n-j}(\tau\lambda) F_\omega(\lambda) d\lambda$ in (3.11), which will be applied in this work. We present the quadrature points $\lambda_k^{(\ell)}$ and weights $w_k^{(\ell)}$ used in (3.11).

- For the trapezoidal rule based on the optimal Talbot contour (see [34]), the quadrature points $\lambda_k^{(\ell)}$ and weights $w_k^{(\ell)}$ are given by

$$(3.14) \quad \lambda_k^{(\ell)} = z(\theta_k, N/T_\ell), \quad w_k^{(\ell)} = \partial_\theta z(\theta_k, N/T_\ell), \quad \theta_k = \frac{(2k+1)\pi}{2N},$$

where $z(\theta, N) = N(-0.4814 + 0.6443(\theta \cot(\theta) + i0.5653\theta))$. Our numerical results indicate that $N = 30$ works well when $T_\ell = (2B^\ell - 2 + n_0)\tau$ and B is not too large.

- For the trapezoidal rule based on the hyperbolic contour (see [18]), the quadrature points $\lambda_k^{(\ell)}$ and weights $w_k^{(\ell)}$ are given by

$$(3.15) \quad \lambda_k^{(\ell)} = z(\theta_k, \mu_\ell), \quad w_k^{(\ell)} = \partial_\theta z(\theta_k, \mu_\ell), \quad \theta_k = (k + 1/2)\hat{h},$$

where $z(\theta, \mu_\ell) = \mu_\ell(1 - \sin(\psi + i\theta)) + \sigma$ and \hat{h} is a step length parameter that is chosen as $\hat{h} = \pi/N$ in this paper. According to [18], we can choose $\sigma = 0$, $\psi = 0.4\pi$, $\mu_\ell = N/(2T_\ell)$, $T_\ell = (2B^\ell - 2 + n_0)\tau$, and $N = \lceil -\log(\tau^{1-\alpha}\epsilon) \rceil$ for numerical simulations, where ϵ is a given precision. Readers can also refer to [30], where a strategy was proposed to choose the parameters for the hyperbolic contour.

Algorithm 1 Fast calculation of $D_\tau^{(\alpha,n)}u = D_\tau^{(\alpha,n,0,\sigma)}u = \sum_{j=0}^n \omega_{n-j}u_j$, where ω_n satisfies $\omega(p, \alpha, \tau, z) = \sum_{n=0}^\infty \omega_n z^n$, and $\omega(p, \alpha, \tau, z)$ can be defined by (2.5) or (2.6).

Input: The positive integers n_0 , N , and $B \geq 2$, the real number α , the time stepsize τ , the quadrature points $\{\lambda_k^{(\ell)}\}$ and weights $\{w_k^{(\ell)}\}$ defined by (3.14) or (3.15), the coefficients ω_n defined by the generating function $\omega(z) = \omega(p, \alpha, \tau, z)$ (see (2.5) or (2.6)), and the function $F_\omega(\lambda)$ (see (3.7) or (3.9)).

Output: ${}_F D_{\tau, n_0}^{(\alpha,n)}u$.

- For each $n \geq n_0$, find the smallest integer L satisfying $n - n_0 + 1 < 2B^L$.
For $\ell = 1, 2, \dots, L - 1$, determine the integer q_ℓ such that

$$(3.10) \quad b_\ell^{(n)} = q_\ell B^\ell \quad \text{satisfies} \quad n - n_0 + 1 - b_\ell^{(n)} \in [B^{\ell-1}, 2B^\ell - 1].$$

Set $b_0^{(n)} = n - n_0$ and $b_L^{(n)} = 0$.

- Decompose the convolution $\sum_{j=0}^n \omega_{n-j}u_j$ as $\sum_{j=0}^n \omega_{n-j}u_j = \sum_{\ell=0}^L u_n^{(\ell)}$, where $u_n^{(0)} = \sum_{j=n-n_0}^n \omega_{n-j}u_j$ and $u_n^{(\ell)} = \sum_{j=b_\ell^{(n)}}^{b_{\ell-1}^{(n)}-1} \omega_{n-j}u_j$.
- For every $1 \leq \ell \leq L$, approximate $u_n^{(\ell)}$ with $\hat{u}_n^{(\ell)}$, where

$$(3.11) \quad \begin{aligned} u_n^{(\ell)} &= \sum_{j=b_\ell^{(n)}}^{b_{\ell-1}^{(n)}-1} \omega_{n-j}u_j = \frac{\tau}{2\pi i} \int_{\Gamma_\ell} (1 - \tau\lambda)^{-[n-(b_{\ell-1}^{(n)}-1)]} F_\omega(\lambda) y^{(\ell)}(\tau\lambda) d\lambda \\ &\approx \text{Im} \left\{ \sum_{k=-N}^{N-1} w_k^{(\ell)} F_\omega(\lambda_k^{(\ell)}) (1 - \tau\lambda_k^{(\ell)})^{-[n-(b_{\ell-1}^{(n)}-1)]} y(\tau\lambda_k^{(\ell)}) \right\} = \hat{u}_n^{(\ell)} \end{aligned}$$

with $y^{(\ell)}(\tau\lambda)$ given by $y^{(\ell)}(\tau\lambda) = \tau \sum_{j=b_\ell^{(n)}}^{b_{\ell-1}^{(n)}-1} e_{(b_{\ell-1}^{(n)}-1)-j}(\tau\lambda) u_j$. Here $y^{(\ell)}(\tau\lambda) = y(b_{\ell-1}^{(n)}\tau, b_\ell^{(n)}\tau, \tau\lambda)$ is the *backward Euler* approximation to the solution at $t = b_{\ell-1}^{(n)}\tau$ of the linear initial-value problem

$$(3.12) \quad y'(t) = \lambda y(t) + u(t), \quad y(b_\ell^{(n)}\tau) = 0.$$

The quadrature points $\lambda_j^{(\ell)}$ and weights $w_j^{(\ell)}$ are given by (3.14) or (3.15).

- Calculate

$$(3.13) \quad {}_F D_{\tau, n_0}^{(\alpha,n)}u = u_n^{(0)} + \hat{u}_n^{(1)} + \dots + \hat{u}_n^{(L)}$$

with $\hat{u}_n^{(\ell)}$ defined by (3.11).

Due to the symmetry of the trapezoidal rule, Eq. (3.11) can be replaced by $\hat{u}_n^{(\ell)} = \text{Im} \left\{ 2 \sum_{k=0}^{N-1} w_k^{(\ell)} F_\omega(\lambda_k^{(\ell)}) (1 - \tau\lambda_k^{(\ell)})^{-[n-(b_{\ell-1}^{(n)}-1)]} y(\tau\lambda_k^{(\ell)}) \right\}$, so that the computational cost can be halved. The memory requirement and computational cost of the present fast method are about $O(\log n_T)$ and $O(Nn_T \log n_T)$, respectively, when n_T is suitably

large; see also [19, 23, 35, 38].

REMARK 3.1. For the contour integral (1.2) in this work, $e_n(\tau\lambda)$ has a similar property as $\exp(\lambda t_n)$ for $\operatorname{Re}(\lambda) \leq 0$ and $F_\omega(\lambda)$ may have weak singularity. The optimal Talbot contour $z(\theta, N/t)$ derived in [34] works very well for the numerical inverse Laplace transform for a fixed t , where the optimal Talbot contour is obtained by a numerical approach and the machine precision is obtained with $N = 32$. We find that this optimal contour $z(\theta, N/T_\ell)$ still works well for the contour integral in the current work for $t \in [B^{\ell-1}, 2B^\ell]$, see Figure 3.1(b).

3.3. Error analysis. In this subsection, we analyse the error of Algorithm 1. The error of the fast method depends only on the approximation $\hat{\omega}_n$ (see (3.8)) to the contour integral (3.6). We have the following error bound.

THEOREM 3.1. Let $\hat{\omega}_n$ be defined by (3.8), in which $\lambda_j^{(\ell)}$ and $w_j^{(\ell)}$ are given by (3.15), and $F_\omega(\lambda)$ is defined by (3.7) or (3.9). For $t = n\tau$, $n \in [B^{\ell-1}, 2B^\ell]$, and $n \geq b_{\mu\ell}t \geq 1$, there exists a positive constant C independent of τ, n and N such that

$$(3.16) \quad |\hat{\omega}_n - \omega_n| \leq C\tau^\alpha \left[\frac{e^{a_0\mu_\ell t/2}}{e^{2d\pi/h} - 1} + e^{(a_1 - a_2 \cosh(Nh))\mu_\ell t/2} + e^{a_1\mu_\ell t/2} \left(1 + \frac{b_{\mu\ell}t}{2(n-Q)} \cosh(Nh) \right)^{1-n+Q} \right],$$

where Q is chosen such that $(\tau\lambda)^{\alpha-1} \lambda^\alpha F_\omega(\lambda)/(1 - \tau\lambda)^{Q+1}$ is bounded for $\lambda(w) = \mu_\ell(1 - \sin(\psi + iw)) + \sigma$, $-d \leq \operatorname{Im}(w) \leq d$, $0 < \psi - d < \psi + d < \pi/2 - \varphi$, $\psi, d > 0$, and $\varphi < \pi/2$.

Proof. We follow the proof of Theorem 3 in [18] to prove (3.16), the detail is omitted here. See also Theorem 3.1 in [30]. \square

Given a precision ϵ , we can choose suitable parameters, such that $|\hat{\omega}_n - \omega_n| \leq C\tau\epsilon$, see [18, 30]. Combining (3.6), (3.8), and (3.11) yields

$$(3.17) \quad |u_n^{(\ell)} - \hat{u}_n^{(\ell)}| = \left| \sum_{j=b_\ell^{(n)}}^{b_{\ell-1}^{(n)}-1} (\omega_{n-j} - \hat{\omega}_{n-j}) u_j \right| \leq C\tau(b_{\ell-1}^{(n)} - b_\ell^{(n)}) \|u\|_\infty \epsilon,$$

which leads to

$$(3.18) \quad |{}_F D_{\tau, n_0}^{(\alpha, n)} u - D_\tau^{(\alpha, n)} u| \leq Ct_n \|u\|_\infty \epsilon.$$

Denote by

$$(3.19) \quad {}_F D_{\tau, n_0}^{(\alpha, n, m, \sigma)} u = {}_F D_{\tau, n_0}^{(\alpha, n)} u + \tau^{-\alpha} \sum_{j=1}^m w_{n,j}^{(\alpha)} (u_j - u_0),$$

where $w_{n,j}^{(\alpha)}$ is defined as in (2.4). Then from (2.8) and (3.18), the overall discretization error of ${}_F D_{\tau, n_0}^{(\alpha, n, m, \sigma)} u$ is given by

$$(3.20) \quad \begin{aligned} |{}_F D_{\tau, n_0}^{(\alpha, n, m, \sigma)} u - k_{-\alpha} * u(t_n)| &= |{}_F D_{\tau, n_0}^{(\alpha, n)} u - D_\tau^{(\alpha, n)} u + D_\tau^{(\alpha, n, m, \sigma)} u - k_{-\alpha} * u(t_n)| \\ &\leq |{}_F D_{\tau, n_0}^{(\alpha, n)} u - D_\tau^{(\alpha, n)} u| + |D_\tau^{(\alpha, n, m, \sigma)} u - k_{-\alpha} * u(t_n)| \\ &\leq C(\epsilon t_n \|u\|_\infty + \tau^p t_n^{\sigma_{m+1}-p-\alpha} + \tau^{\sigma_{m+1}+1} t_n^{-\alpha-1}). \end{aligned}$$

The trapezoidal rule based on the optimal Talbot contour in [34] works well (see (3.14)), and needs fewer quadrature points to achieve the desired accuracy.

Denote the relative pointwise error $e_n^{(T)}$ as

$$e_n^{(T)} = |{}_F D_{\tau, n_0}^{(\alpha, n)} u - D_{\tau}^{(\alpha, n, 0, \sigma)} u| / |D_{\tau}^{(\alpha, n, 0, \sigma)} u|,$$

where $u(t) = t^2 + t$, $D_{\tau}^{(\alpha, n, 0, \sigma)}$ is defined by (2.4), and ${}_F D_{\tau, n_0}^{(\alpha, n)}$ is obtained from Algorithm 1 based on the Talbot quadrature (see (3.14)). We can similarly define the relative pointwise error $e_n^{(H)}$ based on the hyperbolic contour quadrature (3.15).

Figure 3.1 displays the errors $e_n^{(H)}$ and $e_n^{(T)}$, where we set $\alpha = 0.5$, $\tau = 0.01$, $B = 5$, and $n_0 = 50$ in the computation with the generating function defined by (2.6) and $p = 2$. We can see that the fast method based on both the hyperbolic quadrature and the Talbot quadrature shows highly accurate numerical approximations, and the Talbot quadrature uses fewer quadrature points than that of the hyperbolic contour quadrature defined by (3.15). In [30], a strategy for choosing the parameters for the hyperbolic contour quadrature was proposed, which may help to reduce the number of quadrature points.

If the generating function (2.6) with different p is applied, we obtained similar results to those reported above, which are not shown here. For the generating function defined by (2.5), n_0 needs to be chosen up to 200 for $p = 6$ to ensure high accuracy. One can verify that the present algorithm works well for $\alpha \in (-1, 1)$, these results are not shown here.

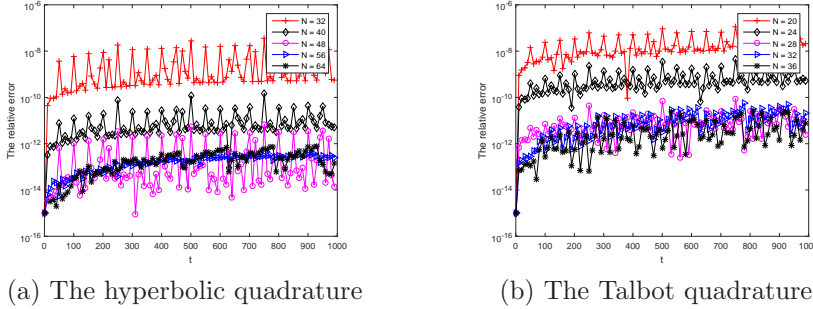


FIG. 3.1. The relative pointwise errors of the fast method based on the hyperbolic contour quadrature and Talbot quadrature, $\alpha = 0.5$, $\tau = 0.01$, $B = 5$.

4. Numerical examples. In this section, two examples are presented to verify the effectiveness of the present semi-implicit and fast method when it is applied to solve nonlinear FDEs. All the algorithms are implemented using MATLAB 2017b, run on a 3.40 GHz PC having 16GB RAM and Windows 7 operating system.

EXAMPLE 4.1. Consider the following scalar FODE

$$(4.1) \quad {}_C D_{0,t}^{\alpha} u(t) = -u(t) + f(u, t), \quad u(0) = u_0, \quad t \in (0, T],$$

where $0 < \alpha \leq 1$ and $f(u, t)$ is a nonlinear function with respect u .

We apply the semi-implicit method (2.17) to solve (4.1), where we set $\lambda = -1$ in (2.17) for this example. We also apply the fully implicit method (2.9) to solve (4.1) for comparison, where the Newton iteration method is used to solve the corresponding nonlinear system. When we say the fast method (2.17) or (2.9) is applied, we mean

that the discrete operator $D_\tau^{(\alpha,n,m,\sigma)}$ in (2.17) or (2.9) is replaced by ${}_F D_{\tau,n_0}^{(\alpha,n,m,\sigma)}$, where ${}_F D_{\tau,n_0}^{(\alpha,n,m,\sigma)}$ is derived using Algorithm 1 (see (3.11)). We always choose the basis $B = 5$, $n_0 = 50$, and $N = 32$ when the fast method based on the Talbot contour is applied. For simplicity, we also set $m_u = m_f = m$ when (2.17) or (2.9) is applied.

The following three cases are considered in this example.

- Case I: For $f = -2u$ and $u_0 = 3$, the exact solution of (4.1) is $u(t) = E_\alpha(-3t^\alpha)$, where $E_\alpha(t) = \sum_{k=0}^{\infty} \frac{t^k}{\Gamma(k\alpha+1)}$ is the Mittag-Leffler function [28].
- Case II: Let $f = -u^2 + g(t)$. Choose a suitable initial condition and $g(t)$ such that the exact solution of (4.1) is $u(t) = 2 + t + t^2/2 + t^3/3 + t^4/4$.
- Case III: Let $f = u(1 - u^2) + 2\cos(2\pi t)$ with the initial condition taken as $u_0 = 1$.

The maximum error is defined by

$$\|e\|_\infty = \max_{0 \leq n \leq T/\tau} |e_n|, \quad e_n = u(t_n) - U_n,$$

where U_n is either the numerical solution from the fast method or the direct method.

The purpose of Case I is to verify the effectiveness of the present semi-implicit and fast method for non-smooth solutions. We demonstrate that adding correction terms improves the accuracy of the numerical solutions significantly, see Tables 4.1 and 4.2, where the maximum relative error and the relative error at $t = 40$ for $\alpha = 0.4$ are displayed. We see that adding correction terms increases the overall accuracy and convergence rate, readers can refer to [7, 21, 39] for related results.

TABLE 4.1

The maximum relative error $\|e\|_\infty/\|u\|_\infty$ of the semi-implicit method (2.17) with fast convolution, Case I, $\sigma_k = k\alpha$, $\alpha = 0.4$, $\kappa = 2$, $B = 5$, $N = 32$, and $T = 40$.

τ	$m = 0$	Order	$m = 1$	Order	$m = 2$	Order	$m = 3$	Order
2^{-7}	7.6319e-2		7.0844e-4		8.2078e-5		6.4330e-5	
2^{-8}	6.4796e-2	0.2361	4.8320e-4	0.5520	4.3412e-5	0.9189	3.2473e-5	0.9862
2^{-9}	5.3713e-2	0.2706	3.1526e-4	0.6161	2.1695e-5	1.0007	1.5317e-5	1.0841
2^{-10}	4.3664e-2	0.2988	1.9873e-4	0.6657	1.0359e-5	1.0664	6.7300e-6	1.1865
2^{-11}	3.4942e-2	0.3215	1.2208e-4	0.7030	4.7706e-6	1.1187	2.8040e-6	1.2631

TABLE 4.2

The relative error $|e_n|/\|u\|_\infty$ of the semi-implicit method (2.17) with fast convolution at $t = 40$, Case I, $\sigma_k = k\alpha$, $\alpha = 0.4$, $\kappa = 2$, $B = 5$, and $N = 32$.

τ	$m = 0$	Order	$m = 1$	Order	$m = 2$	Order	$m = 3$	Order
2^{-7}	1.8929e-6		8.8630e-8		3.4878e-8		1.8337e-8	
2^{-8}	9.4643e-7	1.0000	3.1027e-8	1.5143	1.0813e-8	1.6895	6.6615e-9	1.4609
2^{-9}	4.7322e-7	1.0000	1.0765e-8	1.5272	3.2796e-9	1.7212	2.2083e-9	1.5929
2^{-10}	2.3661e-7	1.0000	3.7238e-9	1.5315	9.7775e-10	1.7460	6.8314e-10	1.6927
2^{-11}	1.1830e-7	1.0000	1.2906e-9	1.5287	2.8842e-10	1.7613	2.0452e-10	1.7400

We now fix the fractional order $\alpha = 0.2$ and let the time stepsize change. In Figure 4.1 (a), we let $\kappa = 0$ and $\tau = 1.4 \times 10^{-3}, 1.5 \times 10^{-3}, 1.59 \times 10^{-3}, 1.6 \times 10^{-3}, 1.7 \times 10^{-3}$ in the computations. We can also see from Table 2.1 that the method (2.17) is stable if $\tau < 1.59 \times 10^{-3}$. We observe that the numerical solutions become unstable when $\tau > 1.59 \times 10^{-3}$. We also observe from Figure 4.1 (b) that the numerical solutions diverge for $\kappa = 0.4$ when $\tau > 1.1 \times 10^{-2}$. These results verify the theoretical findings shown in Table 2.1.

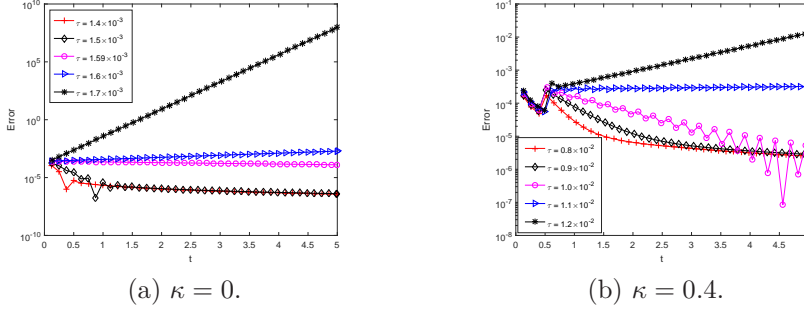


FIG. 4.1. The pointwise errors of the semi-implicit method (2.17) with different time stepsizes, Case I, $\alpha = 0.2, m = 1, B = 5, N = 32$.

For Case II, we solve a nonlinear FODE with $f = -u^2 + g(t)$ and $\partial_u f \in [-434\frac{5}{6}, -4]$ for $t \in [0, 5]$. Here we give a simple guideline for the choice of κ in the method (2.17). From the linear stability analysis of the method (2.17), we have that $\partial_u f$ plays a similar role as ρ does in (2.19), which can be obviously observed from the second semi-implicit method (2.18). Theorem 2.3 provides a practical guideline for selecting κ in real applications, and the stability region of (2.17) becomes larger as κ increases, see Figure 2.2. From (2.22), we can choose $\kappa = \frac{1}{4} \max(-1 - 3\partial_u F) = 325.875$ for the computations. The relative absolute errors $|e^n|/\|u\|_\infty$ at $t = 5$ for different fractional orders are shown in Table 4.3. We can see that the present semi-implicit method exhibits good stability and second-order accuracy for Case II.

TABLE 4.3

The relative error $|e^n|/\|u\|_\infty$ of the semi-implicit method (2.17) with fast convolution at $t = 5$, Case II, $\sigma_1 = 1, m = 1, B = 5, N = 32$.

τ	$\alpha = 0.2$	Order	$\alpha = 0.5$	Order	$\alpha = 0.8$	Order
2^{-5}	2.8685e-4		2.8700e-4		2.8694e-4	
2^{-6}	7.2141e-5	1.9914	7.2180e-5	1.9914	7.2156e-5	1.9915
2^{-7}	1.8089e-5	1.9957	1.8099e-5	1.9957	1.8092e-5	1.9958
2^{-8}	4.5288e-6	1.9979	4.5313e-6	1.9979	4.5296e-6	1.9979
2^{-9}	1.1330e-6	1.9989	1.1337e-6	1.9989	1.1332e-6	1.9989

Next, we fix the stepsize $\tau = 1/256$ and set different $\kappa = 326, 350, 400, 500, 1000$ in the computation for $\alpha = 0.2$ and 0.8 ; the pointwise errors are shown in Figure 4.2. The results shown in Figure 4.2 confirm the theoretical analysis displayed in Theorem 2.3. It can also be observed that very large κ may negatively impact the accuracy of the numerical solutions. One remedy is to use a smaller stepsize, such that κ can be chosen suitably large to ensure both stability and accuracy. Another choice is to use high-order penalty terms $E_q^n(U)$ ($q \geq 3$) in (2.17), but the unconditional stability of the derived method may not be guaranteed even for very large κ , i.e., $q = 3$. Higher order stable semi-implicit methods will be studied in more detail in our future work.

Figures 4.3 (a)–(c) show the numerical solutions for Case III, where the exact solution is not explicitly given. We can see that the solutions are bounded as theoretically expected [31]. Figure 4.3 (d) shows that the fast method is much more efficient than the direct method. We note that the fully implicit method with fast convolution has almost a similar computational cost as the semi-implicit method with fast convolution. Compared with the computational cost from the discrete convolution, the computational cost from the Newton iteration method to obtain the solution in

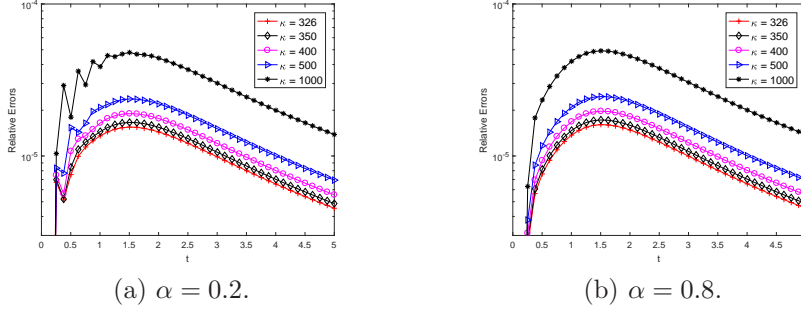


FIG. 4.2. The relative pointwise errors of the semi-implicit method (2.17) with different κ , Case II, $m = 1, B = 5, N = 32$.

the fully implicit method can almost be ignored here, which is different from solving FPDEs as shown in the following example.

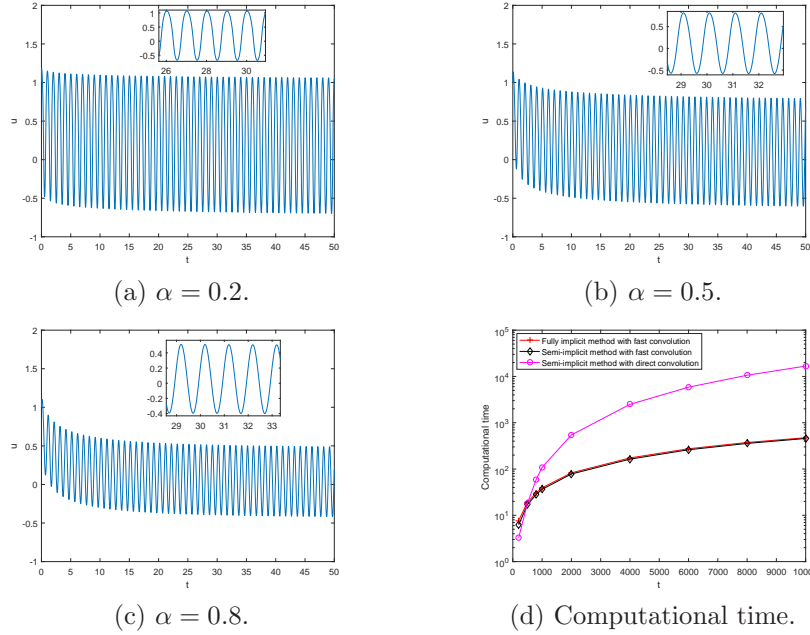


FIG. 4.3. Numerical solutions and the computational cost of different methods, Case II, $\kappa = 3, \tau = 0.005, m = 1, B = 5, N = 32$.

For Case III, we do not know the analytical solution and the reference solutions are obtained using a smaller stepsize $\tau = 2^{-13}$ with two correction terms. Table 4.4 shows the relative error at $t = 50$ with one correction term, where second-order accuracy is observed for different fractional orders.

EXAMPLE 4.2. Consider the following system of FPDEs

$$(4.2) \quad \begin{cases} {}^C D_{0,t}^{\alpha_1} u(t) = \mu_1 \Delta u(t) + f(u, v, x, y, t), \\ {}^C D_{0,t}^{\alpha_2} w(t) = \mu_2 \Delta v(t) + g(u, v, x, y, t) \end{cases}$$

subject to the homogenous boundary conditions, where $0 < \alpha_1, \alpha_2 \leq 1$, $\mu_1, \mu_2 > 0$,

TABLE 4.4

The relative error $|e_n|/\|u\|_\infty$ of the semi-implicit method (2.17) with fast convolution at $t = 50$, Case III, $\sigma_k = k\alpha$, $m = 1$, $\kappa = 3$, $B = 5$, and $N = 32$.

τ	$\alpha = 0.1$	Order	$\alpha = 0.2$	Order	$\alpha = 0.5$	Order	$\alpha = 0.8$	Order
2^{-5}	1.1791e-2		1.2422e-2		1.8310e-2		1.3701e-2	
2^{-6}	2.8763e-3	2.0354	3.4744e-3	1.8381	5.3884e-3	1.7647	2.8694e-3	2.2555
2^{-7}	7.2408e-4	1.9900	8.6976e-4	1.9981	1.3788e-3	1.9664	6.4843e-4	2.1458
2^{-8}	1.8166e-4	1.9949	2.1738e-4	2.0004	3.5033e-4	1.9767	1.5312e-4	2.0823
2^{-9}	4.5338e-5	2.0025	5.4153e-5	2.0051	8.8143e-5	1.9903	3.7019e-5	2.0483

$u(t) = u(x, y, t)$, $v(t) = v(x, y, t)$, and $(x, y, t) \in (0, 1) \times (0, 1) \times (0, T]$. The initial conditions are taken as $u(0) = u(x, y, 0) = u_0(x, y)$ and $v(0) = v(x, y, 0) = v_0(x, y)$.

We focus on the three time-stepping methods for (4.2); the 2D space is discretized using the standard second-order finite volume method (FVM) based on a uniform grid. The second-order generating function $\omega(2, \alpha, \tau, z) = \left(\frac{1-z}{\tau}\right)^\alpha \left(1 + \frac{\alpha}{2} - \frac{\alpha}{2}z\right)$ is applied, see (2.6). For simplicity, no correction terms are applied in this example.

We first make a slight modification of the semi-implicit time-stepping method (2.17) to (4.2), which yields the following semi-discrete method (see (2.25))

$$(4.3) \quad \begin{cases} D_\tau^{(\alpha_1, n, 0, \sigma)} U = \mu_1 \Delta U_n + F_n - E_2^n(F) - \kappa_1 E_2^n(U), \\ D_\tau^{(\alpha_2, n, 0, \sigma)} V = \mu_2 \Delta V_n + G_n - E_2^n(G) - \kappa_2 E_2^n(V), \end{cases}$$

where $F_n = f(U_n, V_n, x, y, t_n)$, $G_n = g(U_n, V_n, x, y, t_n)$, $D_\tau^{(\alpha, n, 0, \sigma)}$ is defined by (2.4), and E_2^n is defined by (2.14).

Applying the FVM to the space discretization of each equation in (4.3), we obtain the fully discrete semi-implicit FVM with direct convolution. If $D_\tau^{(\alpha_k, n, 0, \sigma)}$ in (4.3) is replaced by ${}_F D_{n_0, \tau}^{(\alpha_k, n, 0, \sigma)}$, where ${}_F D_{n_0, \tau}^{(\alpha_k, n, 0, \sigma)}$ is defined by (3.19), then the fully discrete semi-implicit FVM with fast convolution is derived. The fully discrete implicit FVM with direct convolution can be derived by applying the time discretization (2.9) to each equation of (4.3) with space approximated by the FVM. When the new fast method is applied, we always set $B = 5$, $n_0 = 50$, $N = 32$.

- Case I: Let $u_0 = v_0 = \sin(\pi x) \sin(\pi y)$, $f = -vu^2 + \hat{f}(x, y, t)$, and $g = -v^2u + \hat{g}(x, y, t)$. Choose suitable \hat{f} and \hat{g} such that the exact solution to (4.2) is

$$u = E_{\alpha_1}(-t^{\alpha_1}) \sin(\pi x) \sin(\pi y), \quad v = E_{\alpha_2}(-t^{\alpha_2}) \sin(\pi x) \sin(\pi y).$$

- Case II: Let $u_0 = x(1-x)y(1-y)$, $v_0 = \sin(\pi x) \sin(\pi y)$, $f = -u^2v$, and $g = -v^2u$.

Table 4.5 compares the efficiency and accuracy of the implicit FVM and the semi-implicit FVM for Case I, in which the nonlinear algebraic system arising due to the coupling of the implicit FVM is solved by fixed point iteration. Obviously, the semi-implicit method is faster than the implicit method, but is a little less accurate than the implicit method, which can be explained from the truncation error R^n of the semi-implicit method defined by (2.16), i.e., $R^n = O(\tau^2 t_n^{\sigma_1 - 2 - \alpha}) + O(\tau^{\sigma_1 + 1} t_n^{-\alpha - 1}) + O(\tau^2 t_n^{\delta_1 - 2}) + O(\tau^2 t_n^{\sigma_1 - 2})$. The time truncation error of the implicit method contains only the first two terms of R^n . However, the truncation error of the semi-implicit method also contains the third and fourth terms of R^n that may play dominant roles here, which leads to a little less accurate numerical solution of the semi-implicit method. Because of the symmetry, the same accuracy of the numerical solutions of u and v are observed.

TABLE 4.5

Comparison of the semi-implicit FVM and the implicit FVM at $t = 2$, Case I, $\mu_1 = \mu_2 = 1$, $\alpha_1 = \alpha_2 = 0.5$, $\kappa_1 = \kappa_2 = 2$, and $h = 1/256$.

$1/\tau$	Semi-implicit method			Fully implicit method		
	L^2 -error(u)	L^2 -error(v)	Time(s)	L^2 -error(u)	L^2 -error(v)	Time(s)
8	8.8202e-4	8.8202e-4	0.7331	5.9450e-5	5.9450e-5	3.3517
16	2.2203e-4	2.2203e-4	1.5142	2.6788e-5	2.6788e-5	6.5332
32	5.6555e-5	5.6555e-5	3.4880	1.3454e-5	1.3454e-5	13.318
48	2.4377e-5	2.4377e-5	5.9117	9.7126e-6	9.7126e-6	20.602
64	1.2608e-5	1.2608e-5	8.7127	8.0249e-6	8.0249e-6	27.735

We compare in Table 4.6 the semi-implicit direct method with the semi-implicit fast method for Case I. Clearly, the two methods achieve almost similar numerical solutions. This can be explained from the fact that the time discretization error of the fast method contains two parts, one part is the same as that of the direct method, the other part is from the quadrature to discretize the contour integral, which is independent of and also far smaller than the first part due to the sufficient number of quadrature points, see related results shown in Figure 3.1(b). The fast method is much more efficient than the direct method. “Out of memory” occurred for the direct method when $t > 1200$, while the fast method works for $t \gg 1200$ and the computational cost increases almost linearly, see Table 4.6. Theoretically, the computational time of the direct method increases proportional to n_T^2 , so the computational time at $t = 400$ is about 4×19207.5798 seconds, but we did not obtain the results within the expected time due to the memory problem.

TABLE 4.6

Comparison of the semi-implicit method with direct convolution and fast convolution, Case I, $\alpha_1 = 0.2$, $\alpha_2 = 0.8$, $h = 1/128$, $\tau = 0.01$, and $\kappa_1 = \kappa_2 = 2$.

t	Direct convolution			Fast convolution		
	L^2 -error(u)	L^2 -error(v)	Time(s)	L^2 -error(u)	L^2 -error(v)	Time(s)
40	7.0926e-6	2.5317e-7	1253.9869	7.0926e-6	2.5317e-7	994.6982
100	6.4289e-6	1.4192e-7	4849.6792	6.4289e-6	1.4192e-7	2618.0711
200	5.7959e-6	8.0380e-8	19207.5798	5.7959e-6	8.0380e-8	5463.2218
300	5.7810e-8	5.7810e-8	43056.7172	5.7810e-8	5.7810e-8	7954.6040
400	-	-	-	5.2029e-6	4.5797e-8	11330.6522
1000	-	-	-	4.4865e-6	2.1880e-8	29548.2192
2000	-	-	-	3.9966e-6	1.2539e-8	60915.4783

For Case II, we do not have an explicit form of the analytical solution, we show numerical solutions in Figures 4.4 and 4.5. Figures 4.4 (a) and (b) display, respectively, the numerical solutions of u and v at $t = 50$ for $(\alpha_1, \alpha_2) = (0.8, 0.2)$. Figures 4.4 (c) and (d) show numerical solutions of u and v at different times with $y = 0.5$, we see that the numerical solutions decay as time evolves, see also Figure 4.5. For other fractional orders, similar behavior can be observed, see Figures 4.5 (a) and (b) for $\alpha_1 = \alpha_2 = 0.5$.

5. Conclusion and discussion. In this paper, we considered how to efficiently solve nonlinear time-fractional differential equations. The nonlinearity is resolved by proposing a new class of semi-implicit time-stepping methods. The stability of the new semi-implicit methods was investigated, and the stability interval was theoretically given and verified numerically. In particular, several cases of the semi-implicit methods are unconditionally stable by choosing parameters that are explicitly given.

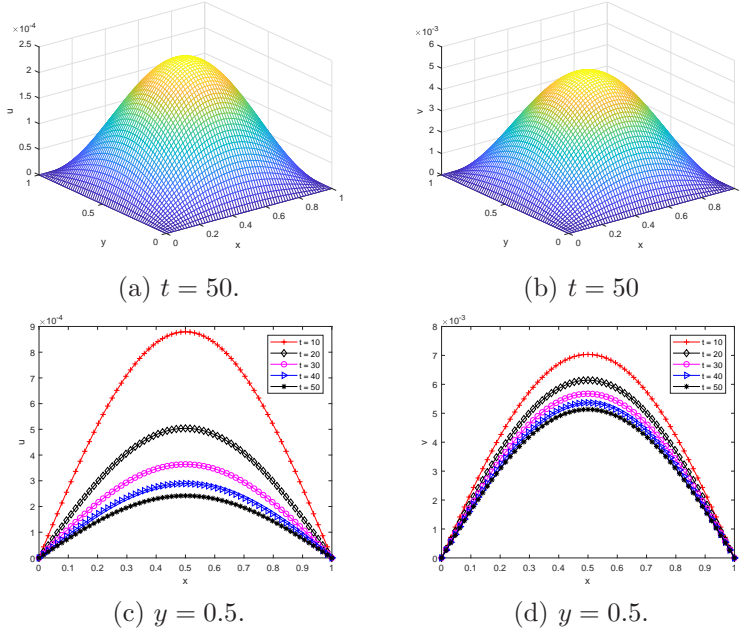


FIG. 4.4. Numerical solutions for Case II, $\alpha_1 = 0.8, \alpha_2 = 0.2, \kappa_1 = \kappa_2 = 2, \tau = 0.01, h = 1/64, B = 5, N = 32$.

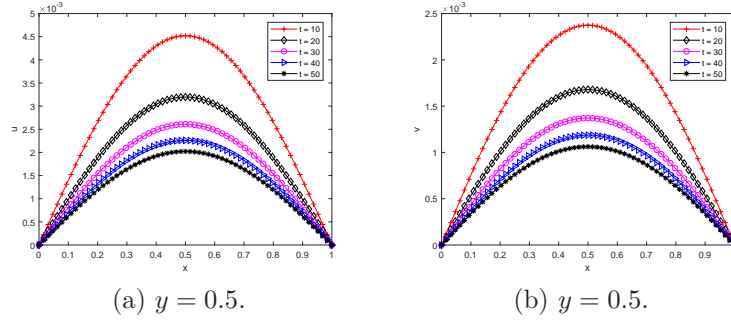


FIG. 4.5. Numerical solutions for Case II, $\alpha_1 = \alpha_2 = 0.5, \kappa_1 = \kappa_2 = 2, \tau = 0.01, h = 1/64, B = 5, N = 32$.

We also extend the semi-implicit methods for a scalar equation to a system of equations with the stability condition given theoretically.

The nonlocality of the fractional operator leads to a discrete convolution, which is costly by direct computation. This issue is resolved by the new fast and memory-saving algorithm. The new approach simplifies and extends the method in [30] to a wider class of discrete convolution methods for approximating the fractional operator with coefficients generated from the generating functions [21]. We prove that the error originating from the fast calculation can be arbitrarily small and is independent of the truncation error of the direct method. In the fast method, a series of ODEs with homogenous initial conditions need to be solved at each time step. These ODEs were solved by the multi-step method that corresponds to the fractional multi-step method for the fractional operator in [30]. However, in the current work, these ODEs

are solved using the *backward Euler* method. If the k -step ($k > 1$) method is applied, then additional errors may occur since k initial values are needed to start the ODE solver, but only one initial value is known.

The semi-implicit methods in the present work achieve at most second-order accuracy, even though a high-order time-stepping method for the fractional operator is applied. In future work, we will consider how to construct uniformly stable high-order semi-implicit methods for nonlinear time-fractional differential equations. Another computational issue is to seek a uniform quadrature with high accuracy to discretize the integral contour (3.3), which will make it easier to implement the present fast method similarly to those given in [2, 15, 17].

Appendix A. Proofs of Theorems 2.1 and 2.2. Proof of Theorem 2.1.

Proof. Denote by $U(z) = \sum_{n=0}^{\infty} U_n z^n$, $|z| \leq 1$. We have from (2.20)

$$\sum_{n=2}^{\infty} \sum_{j=0}^n \omega_{n-j}^{(\alpha)} (U_j - U_0) z^n = (\lambda - \kappa) \tau^{\alpha} \sum_{n=2}^{\infty} U_n z^n + (\rho + \kappa) \tau^{\alpha} \sum_{n=2}^{\infty} (2U_{n-1} - U_{n-2}) z^n,$$

which leads to

$$\begin{aligned} (A.1) \quad & \omega(p, \alpha, 1, z) U(z) - \omega_0^{(\alpha)} U_0 - (\omega_0^{(\alpha)} U_1 + \omega_1^{(\alpha)} U_0) z - U_0 \sum_{n=2}^{\infty} \sum_{j=0}^n \omega_j^{(\alpha)} z^n \\ & = (\lambda - \kappa) \tau^{\alpha} (U(z) - U_0 - U_1 z) + (\rho + \kappa) \tau^{\alpha} (2z(U(z) - U_0) - z^2 U(z)), \end{aligned}$$

where we have used the following property

$$\omega(p, \alpha, 1, z) U(z) = \sum_{n=0}^{\infty} \sum_{j=0}^n \omega_{n-j}^{(\alpha)} U_j z^n.$$

Rewrite (A.1) into the following form

$$(A.2) \quad U(z) = \frac{H(z)}{\omega(p, \alpha, 1, z) - \tau^{\alpha}(\lambda + \rho) + \tau^{\alpha}(\rho + \kappa)(1 - z)^2},$$

where $H(z) = \sum_{n=0}^{\infty} H_n z^n$. According to Eq. (3.3) and Lemma 3.5 in [21], one has $\sum_{j=0}^n \omega_j^{(\alpha)} = \frac{n^{-\alpha}}{\Gamma(1-\alpha)} + O(n^{-\alpha-1})$, which yields $H_n = O(n^{-\alpha})$. On the other hand, we have $\omega(p, \alpha, 1, z) - \tau^{\alpha}(\lambda + \rho) + \tau^{\alpha}(\rho + \kappa)(1 - z)^2 = \sum_{n=0}^{\infty} Q_n z^n = Q(z)$ with $Q_n = O(n^{-\alpha-1})$, where $\omega_n^{(\alpha)} = O(n^{-\alpha-1})$ has been used [21]. According to [22], $U_n \rightarrow 0$ as $n \rightarrow \infty$ if $Q(z) \neq 0, |z| \leq 1$, i.e., the method is stable if $\tau^{\alpha} \neq \frac{\omega(p, \alpha, 1, z)}{(\lambda + \rho) - (\rho + \kappa)(1 - z)^2}, |z| \leq 1$. The proof is complete. \square

Proof of Theorem 2.2.

Proof. Lemma 3.5 and Eq. (3.3) in [21] yield

$$\sum_{j=0}^n \omega_{n-j}^{(\alpha)} j^{\sigma_k} = \frac{n^{\sigma_k - \alpha}}{\Gamma(1 + \sigma_k - \alpha)} + O(n^{\sigma_k - \alpha - p}) + O(n^{-\alpha - 1}),$$

which leads to

$$\sum_{j=1}^m w_{n,j}^{(\alpha)} j^{\sigma_k} = O(n^{\sigma_k - \alpha - p}) + O(n^{-\alpha - 1}), \quad 1 \leq k \leq m.$$

The above linear system implies that the starting weights $w_{n,j}^{(\alpha)}$ in (2.4) satisfy

$$w_{n,j}^{(\alpha)} = O(n^{\sigma_1 - \alpha - p}) + O(n^{\sigma_2 - \alpha - p}) + \dots + O(n^{\sigma_m - \alpha - p}) + O(n^{-\alpha - 1}).$$

By the same reasoning, we can obtain that the starting weights $w_{n,j}^{(f)}$ and $w_{n,j}^{(u)}$ used in (2.12) satisfy

$$\begin{aligned} w_{n,j}^{(u)} &= O(n^{\sigma_1 - q}) + O(n^{\sigma_2 - q}) + \dots + O(n^{\sigma_{m_u} - q}), \\ w_{n,j}^{(f)} &= O(n^{\delta_1 - q}) + O(n^{\delta_2 - q}) + \dots + O(n^{\delta_{m_f} - q}). \end{aligned}$$

Denote $m_{\max} = \max\{m, m_u, m_f\} + 1$ and

$$U(z) = \sum_{n=m_{\max}}^{\infty} U_n z^n.$$

For the method (2.17) with correction terms, we can similarly derive

$$(A.3) \quad U(z) = \frac{H(z) + \hat{H}(z)}{\omega(p, \alpha, 1, z) - \tau^\alpha(\lambda + \rho) + \tau^\alpha(\rho + \kappa)(1 - z)^2},$$

where $H(z)$ is similarly derived as in (A.2) with $H_n \rightarrow 0$ as $n \rightarrow \infty$, $\hat{H}(z) = \sum_{n=0}^{\infty} \hat{H}_n z^n$, $\hat{H}_n = 0, 0 \leq n \leq m_{\max}$, and

$$\hat{H}_n = - \sum_{j=1}^m w_{n,j}^{(\alpha)}(U_j - U_0) + \rho \tau^\alpha \sum_{j=1}^{m_f} w_{n,j}^{(f)}(U_j - U_0) + \kappa \tau^\alpha \sum_{j=1}^{m_u} w_{n,j}^{(u)}(U_j - U_0)$$

for $n \geq m_{\max}$. Obviously, $\hat{H}_n \rightarrow 0$ as $n \rightarrow \infty$ if

$$\sigma_k - \alpha - p < 0, \quad \sigma_{m_u} - q < 0, \quad \sigma_{m_f} - q < 0.$$

The above inequalities yield Theorem 2.2, which ends the proof. \square

Appendix B. Proof of Theorem 2.3. We prove Theorem 2.3 for $p = q = 2$ with $\omega(2, \alpha, 1, z) = \tau^\alpha \omega(2, \alpha, \tau, z) = (1 - z)^\alpha (1 + \frac{\alpha}{2} - \frac{\alpha}{2}z)$, other cases can be similarly proved. The following notations are used to simplify the proof, i.e.,

$$(B.1) \quad \begin{aligned} D &= \{(x, y) | x^2 + y^2 < 1\}, \quad \partial D = \{(x, y) | x^2 + y^2 = 1\}, \\ D_U &= \{(x, y) | x^2 + y^2 < 1, 0 < y < 1\}, \quad \partial D_U = \partial D_U^{(1)} \cup \partial D_U^{(2)}, \end{aligned}$$

where $\partial D_U^{(1)} = \{(x, y) | -1 \leq x \leq 1, y = 0\}$, $\partial D_U^{(2)} = \{(x, y) | x^2 + y^2 = 1, |x| < 1, 0 < y < 1\}$. Denote $\bar{D} = D \cup \partial D$ and $\bar{D}_U = D_U \cup \partial D_U$. Then, D_U is the interior of the upper semi-circular domain with boundary ∂D_U . We can similarly define the lower semi-circular domain \bar{D}_L . The proof of Theorem 2.3 is equivalent to proving that $f(z) = \frac{\omega(2, \alpha, 1, z)}{\lambda - \kappa + (\rho + \kappa)(2z - z^2)}$ is not positive real for $z \in \bar{D}$. We just need to prove that $f(z)$ is not positive real for $z \in \bar{D}_U$, which also holds for $z \in \bar{D}_L$ by the same reasoning.

Proof. For simplicity, we denote $W(x, y) = (1 - z)^\alpha (1 + \frac{\alpha}{2} - \frac{\alpha}{2}z)$, and $V(x, y) = \lambda - \kappa + (\rho + \kappa)(2z - z^2)$, where $z = x + iy = r \exp(i\theta)$, $i^2 = -1$, $\theta \in [-\pi, \pi]$, $0 \leq r \leq 1$.

Denote $W(x, y) = W_1(x, y) + iW_2(x, y)$ and $V(x, y) = V_1(x, y) + iV_2(x, y)$, where W_1, W_2, V_1, V_2 are real. Then we have

$$(B.2) \quad \begin{cases} W_1(x, y) \geq 0, & |x|^2 + |y|^2 \leq 1, \\ W_2(\cos \theta, \sin \theta) \geq 0, & \theta \in [-\pi, 0], \\ W_2(\cos \theta, \sin \theta) \leq 0, & \theta \in [0, \pi]. \end{cases}$$

The first inequality can be found in [33]. Let $\phi(\theta) = \left(2 \sin \frac{\theta}{2}\right)^\alpha$. Then we have $W_2(\cos \theta, \sin \theta) = \phi(-\theta) \left[\left(1 + \frac{\alpha}{2} - \frac{\alpha}{2} \cos \theta\right) \sin \frac{\alpha}{2}(\theta + \pi) - \frac{\alpha}{2} \cos \frac{\alpha}{2}(\theta + \pi) \sin(\theta) \right] > 0$, $\theta \in (-\pi, 0)$. The third inequality in (B.2) can be similarly derived from $W_2(\cos \theta, \sin \theta) = \phi(\theta) \left[\left(1 + \frac{\alpha}{2} - \frac{\alpha}{2} \cos \theta\right) \sin \frac{\alpha}{2}(\theta - \pi) - \frac{\alpha}{2} \cos \frac{\alpha}{2}(\theta - \pi) \sin \theta \right] < 0$, $\theta \in (0, \pi)$.

For V_1 and V_2 , we have the following results.

$$(B.3) \quad \begin{cases} V_1(x, y) < 0, & \frac{\lambda - 3\rho}{4} < \kappa < -2\lambda - 3\rho, \quad |x|^2 + |y|^2 \leq 1, \\ V_2(\cos \theta, \sin \theta) \leq 0, & \kappa > -\rho, \quad \theta \in [-\pi, 0], \\ V_2(\cos \theta, \sin \theta) \geq 0, & \kappa > -\rho, \quad \theta \in [0, \pi]. \end{cases}$$

The first inequality in (B.3) can be derived by checking $\widehat{V}_1(\pm 1) < 0$ and $\widehat{V}_1(1/2) < 0$, where $\widehat{V}_1(\cos \theta) = V_1(\cos \theta, \sin \theta) = \lambda - \kappa + (\rho + \kappa)(2 \cos \theta - 2 \cos^2 \theta + 1)$. The second and third inequalities in (B.3) can be easily deduced from $V_2(\cos \theta, \sin \theta) = (\rho + \kappa)(2 \sin \theta - \sin 2\theta) = 2(\rho + \kappa) \sin \theta(1 - \cos \theta)$.

Next, we prove that $f(z) = \frac{\omega(2, \alpha, 1, z)}{\psi_2(z)} = \frac{W(x, y)}{V(x, y)}$ cannot be positive real on \bar{D}_U .

- Step 1) Assume that $\frac{\lambda - 3\rho}{4} < \kappa < -2\lambda - 3\rho$ and there exists a positive constant $c > 0$, such that $f(z) = \frac{W_1 + iW_2}{V_1 + iV_2} = c$. Then we have $W_1 - cV_1 = 0$. Eqs. (B.2) and (B.3) imply $W_1 - cV_1 > 0$ for all $|z| \leq 1$, which yields a contradiction. Therefore, $f(z)$ cannot be a positive real number when $\frac{\lambda - 3\rho}{4} < \kappa < -2\lambda - 3\rho$.
- Step 2) Since $\omega(2, \alpha, 1, z)$ is analytic for $|z| < 1$ and continuous for $|z| = 1$, the imaginary part $W_2(x, y)$ of $\omega(2, \alpha, 1, z)$ is a harmonic function in the interior of the unit circular domain \bar{D} and is continuous on the boundary ∂D of \bar{D} . It implies that $W_2(x, y)$ (or $V_2(x, y)$) is also analytic in D_U and continuous on ∂D_U . Therefore, W_2 (or V_2) attains its maximum and minimum value on the boundary \bar{D}_U . From (B.2) and (B.3), we have $W_2(x, y) \geq 0$ and $V_2(x, y) \leq 0$ for $(x, y) \in \bar{D}_U$ if $\kappa > -\rho$. For any $(x, y) \in \bar{D}_U \setminus \partial D_U^{(1)}$, we assume that there exists a positive number c such that $f(z) = \frac{W_1 + iW_2}{V_1 + iV_2} = c$, which leads to $W_2 - cV_2 = 0$. On the other hand, we have $V_2(x, y) = (\rho + \kappa)2r \sin \theta(1 - r \cos \theta) > 0$ for $(x, y) = (r \cos \theta, r \sin \theta) \in \bar{D}_U \setminus \partial D_U^{(1)}$, which yields $0 = W_2 - cV_2 < 0$. Therefore, $f(z)$ cannot be positive real for $z = (x, y) \in \bar{D}_U \setminus \partial D_U^{(1)}$. If $(x, y) \in \partial D_U^{(1)}$, then $f(z)$ is real and $f(z) = \frac{W_1}{V_1} \leq 0$ due to the fact $W_1 \geq 0$ and $V_1 < 0$. Therefore, $f(z)$ is not positive real on \bar{D}_U if $\kappa > -\rho$.

From Steps 1) and 2), we prove that $f(z)$ is not positive real on \bar{D}_U if $\kappa > \frac{\lambda - 3\rho}{4}$. We can similarly prove that $f(z)$ is not positive real on \bar{D}_L if $\kappa < -2\lambda - 3\rho$. Hence, $f(z)$ is not positive real for $|z| \leq 1$, which implies the stability region \mathbb{S} defined (2.21) contains the interval $(0, \infty)$. The proof is completed. \square

Appendix C. The authors wish to thank the referees for their constructive comments and suggestions, which greatly improve the quality of this paper.

REFERENCES

- [1] U. M. ASCHER, S. J. RUUTH, AND B. T. R. WETTON, *Implicit-explicit methods for time-dependent partial differential equations*, SIAM J. Numer. Anal., 32 (1995), pp. 797–823.
- [2] D. BAFFET AND J. S. HESTHAVEN, *A kernel compression scheme for fractional differential equations*, SIAM J. Numer. Anal., 55 (2017), pp. 496–520.
- [3] L. BANJAI, M. LÓPEZ-FERNÁNDEZ, AND A. SCHÄDLE, *Fast and oblivious algorithms for dissipative and two-dimensional wave equations*, SIAM J. Numer. Math., 55 (2017), pp. 621–639.
- [4] W. CAO, F. ZENG, Z. ZHANG, AND G. E. KARNIADAKIS, *Implicit-explicit difference schemes for nonlinear fractional differential equations with nonsmooth solutions*, SIAM J. Sci. Comput., 38 (2016), pp. A3070–A3093.
- [5] W. CAO, Z. ZHANG, AND G. E. KARNIADAKIS, *Time-splitting schemes for fractional differential equations I: Smooth solutions*, SIAM J. Sci. Comput., 37 (2015), pp. A1752–A1776.
- [6] K. DIETHELM, *The analysis of fractional differential equations*, vol. 2004 of Lecture Notes in Mathematics, Springer-Verlag, Berlin, 2010. An application-oriented exposition using differential operators of Caputo type.
- [7] K. DIETHELM, J. M. FORD, N. J. FORD, AND M. WEILBEER, *Pitfalls in fast numerical solvers for fractional differential equations*, J. Comput. Appl. Math., 186 (2006), pp. 482–503.
- [8] K. DIETHELM, N. J. FORD, AND A. D. FREED, *Detailed error analysis for a fractional Adams method*, Numer. Algorithms, 36 (2004), pp. 31–52.
- [9] N. J. FORD, M. L. MORGADO, AND M. REBELO, *Nonpolynomial collocation approximation of solutions to fractional differential equations*, Fract. Calc. Appl. Anal., 16 (2013), pp. 874–891.
- [10] L. GALEONE AND R. GARRAPPA, *Fractional Adams-Moulton methods*, Math. Comput. Simulation, 79 (2008), pp. 1358–1367.
- [11] L. GALEONE AND R. GARRAPPA, *Explicit methods for fractional differential equations and their stability properties*, J. Comput. Appl. Math., 228 (2009), pp. 548–560.
- [12] R. GARRAPPA, *On some explicit Adams multistep methods for fractional differential equations*, J. Comput. Appl. Math., 229 (2009), pp. 392–399.
- [13] R. GARRAPPA, *On linear stability of predictor-corrector algorithms for fractional differential equations*, Int. J. Comput. Math., 87 (2010), pp. 2281–2290.
- [14] R. GARRAPPA, *Trapezoidal methods for fractional differential equations: Theoretical and computational aspects*, Math. Comput. Simulation, 110 (2015), pp. 96–112.
- [15] S. JIANG, J. ZHANG, Q. ZHANG, AND Z. ZHANG, *Fast evaluation of the Caputo fractional derivative and its applications to fractional diffusion equations*, Commun. Comput. Phys., 21 (2017), pp. 650–678.
- [16] G. E. KARNIADAKIS, M. ISRAELI, AND S. A. ORSZAG, *High-order splitting methods for the incompressible Navier–Stokes equations*, J. Comput. Phys., 97 (1991), pp. 414–443.
- [17] J.-R. LI, *A fast time stepping method for evaluating fractional integrals*, SIAM J. Sci. Comput., 31 (2010), pp. 4696–4714.
- [18] M. LÓPEZ-FERNÁNDEZ, C. LUBICH, C. PALENCIA, AND A. SCHÄDLE, *Fast Runge–Kutta approximation of inhomogeneous parabolic equations*, Numer. Math., 102 (2005), pp. 277–291.
- [19] M. LÓPEZ-FERNÁNDEZ, C. LUBICH, AND A. SCHÄDLE, *Adaptive, fast, and oblivious convolution in evolution equations with memory*, SIAM J. Sci. Comput., 30 (2008), pp. 1015–1037.
- [20] C. LUBICH, *Runge–Kutta theory for Volterra and Abel integral equations of the second kind*, Math. Comp., 41 (1983), pp. 87–102.
- [21] C. LUBICH, *Discretized fractional calculus*, SIAM J. Math. Anal., 17 (1986), pp. 704–719.
- [22] C. LUBICH, *A stability analysis of convolution quadratures for Abel–Volterra integral equations*, IMA J. Numer. Anal., 6 (1986), pp. 87–101.
- [23] C. LUBICH AND A. SCHÄDLE, *Fast convolution for nonreflecting boundary conditions*, SIAM J. Sci. Comput., 24 (2002), pp. 161–182.
- [24] Y. LUCHKO, *Initial-boundary problems for the generalized multi-term time-fractional diffusion equation*, J. Math. Anal. Appl., 374 (2011), pp. 538–548.
- [25] W. MCLEAN, *Fast summation by interval clustering for an evolution equation with memory*, SIAM J. Sci. Comput., 34 (2012), pp. A3039–A3056.
- [26] R. METZLER AND J. KLAFTER, *The random walk’s guide to anomalous diffusion: a fractional dynamics approach*, Phys. Rep., 339 (2000), pp. 1–77.
- [27] L. PARESCHI AND G. RUSSO, *Implicit–explicit Runge–Kutta schemes and applications to hyperbolic systems with relaxation*, J. Sci. Comput., 25 (2005), pp. 129–155.
- [28] I. PODLUBNY, *Fractional differential equations*, Academic Press, Inc., San Diego, CA, 1999.
- [29] S. G. SAMKO, A. A. KILBAS, AND O. I. MARICHEV, *Fractional integrals and derivatives*, Gordon and Breach Science Publishers, Yverdon, 1993.
- [30] A. SCHÄDLE, M. LÓPEZ-FERNÁNDEZ, AND C. LUBICH, *Fast and oblivious convolution quadrature*, SIAM J. Sci. Comput., 28 (2006), pp. 421–438.

- [31] D. WANG AND A. XIAO, *Dissipativity and contractivity for fractional-order systems*, Nonlinear Dynamics, 80 (2015), pp. 287–294.
- [32] H. WANG AND T. S. BASU, *A fast finite difference method for two-dimensional space-fractional diffusion equations*, SIAM J. Sci. Comput., 34 (2012), pp. A2444–A2458.
- [33] Z. WANG AND S. VONG, *Compact difference schemes for the modified anomalous fractional sub-diffusion equation and the fractional diffusion-wave equation*, J. Comput. Phys., 277 (2014), pp. 1–15.
- [34] J. A. C. WEIDEMAN, *Optimizing Talbot’s contours for the inversion of the Laplace transform*, SIAM J. Numer. Anal., 44 (2006), pp. 2342–2362.
- [35] Y. YU, P. PERDIKARIS, AND G. E. KARNIADAKIS, *Fractional modeling of viscoelasticity in 3D cerebral arteries and aneurysms*, J. Comput. Phys., 323 (2016), pp. 219–242.
- [36] S. B. YUSTE, *Weighted average finite difference methods for fractional diffusion equations*, J. Comput. Phys., 216 (2006), pp. 264–274.
- [37] S. B. YUSTE AND L. ACEDO, *An explicit finite difference method and a new von Neumann-type stability analysis for fractional diffusion equations*, SIAM J. Numer. Anal., 42 (2005), pp. 1862–1874.
- [38] F. ZENG, I. TURNER, AND K. BURRAGE, *A stable fast time-stepping method for fractional integral and derivative operators*, J. Sci. Comput., 2018, in press.
- [39] F. ZENG, Z. ZHANG, AND G. E. KARNIADAKIS, *Second-order numerical methods for multi-term fractional differential equations: Smooth and non-smooth solutions*, Comput. Methods Appl. Mech. Engrg., 327 (2017), pp. 478–502.